FORSCHUNGSZENTRUM
ROSSENDORF e.V.

FZR

FZR Preprint 93 - 01
February 1993

W. Iskra, M. Müller, I. Rotter

Selforganization in the nuclear system

I: The slaving principle

Selforganization in the nuclear system I: The slaving principle

W. Iskra [1], M. Müller and I. Rotter [2]

Forschungszentrum Rossendorf
Institut für Kern- und Hadronenphysik
O-8051 Dresden, Germany

Abstract

The properties of the atomic nucleus are investigated from the point of view of selforganization. The nucleus is described as an open quantum mechanical many-body system embedded in the continuum of decay channels. The transition from low to high level density is traced as a function of the coupling strength between the discrete nuclear states and the environment of decay channels. A redistribution inside the nucleus takes place in a small region around some critical value of the coupling strength. As a result of the redistribution, the effective number of degrees of freedom is reduced. The analogy of the results obtained numerically for the nuclear system to the laws of synergetics is investigated. The slaving principle is shown to hold in the open quantum system.

[1] *On leave of absence from:* Soltan Institute for Nuclear Studies, 00-681 Warszawa, Poland

[2] *also:* Technische Universität Dresden, Abteilung Physik, O-8027 Dresden, Germany

1 Introduction

As it is well known, the discrete states of the atomic nucleus at low level density are described well by wavefunctions containing all nucleons in bound single-particle states [1]. As a matter of fact, most excited states have, however, a finite lifetime, i.e. they are embedded in the continuum of decay channels and decay with a certain probability.

In an exact theory, the coupling to the continuum of decay channels has to be taken into account, therefore, from the very beginning. The Schrödinger equation $(H - E)\Psi = 0$ must be solved with an ansatz for Ψ containing not only the discrete states but also the scattering states [2]. The spectroscopic properties are then described in a subspace of the whole function space. In such a formalism, the asymptotic part of the wavefunctions as well as the lifetimes of the states follow immediately from the coupling of the (discrete) states to the environment of decay channels [3].

The equations describing the spectroscopic properties of discrete states are linear as long as we restrict ourselves to the function space of bound states which then we consider as the full Hilbert space. As soon as we consider a function space spanned by bound and scattering states, the equations become *non-linear* because in such a case the function space of discrete states is a *subspace* of the whole function space.

Systems described by non-linear equations are expected to be selforganized. Their properties are determined by the interplay between internal stability and interaction with the environment. This fact, well known from complicated, e.g. biological systems, has been observed also in the open quantum mechanical nuclear system [3].

The evolution of a system can be traced best by investigating its behaviour near instability points in dependence of some control parameter [4]. Here, a selforganizing system which is described by classical methods is shown to form stable modes together with a few unstable modes. The unstable modes determine the behaviour of the system while the stable ones are suppressed ("slaving principle"). By that, the complexity of the system is reduced. Further, the information entropy increases, in this case, up to a certain maximal value as a function of the increasing control parameter in full analogy to the second law of thermodynamics for closed systems ("maximal information entropy principle") [4].

In an open quantum mechanical nuclear system, one can also differentiate between stable and unstable modes [3], although the mathematical formalism

is completely different. At a critical value of the coupling strength between system and environment, a redistribution of the spectroscopic values takes place. Most states of the system become long-lived (trapped) while a few of them are distinguished by large widths. They are the relevant modes at strong coupling [5]. The number of these states, the widths of which are large as a result of the redistribution taking place in the nucleus, is exactly equal to the number of open decay channels [6]. In other words, the environment imprints its properties into the system. The original spectroscopic information is lost. Such a redistribution is observed and investigated by different methods in different quantum systems at high level density [3,5-14]. A similar problem is discussed in quantum chemistry [15].

Our aim is to trace, in this paper, the redistribution in the nucleus taking place at high level density, and to compare the results in detail with those obtained in synergetics [4]. The basic set of wavefunctions is the set of Slater determinants for which the single-particle quantum numbers j and l as well as the total spin J are good quantum numbers. The number of levels is much higher than the number of open decay channels. We focus mainly on the differences in the wavefunctions of trapped and broad modes which occur, in any case, by selforganization at high level density.

In Sect. 2, the model used for the numerical calculations is sketched. The underlying equations are shown to be *non-linear* due to the fact that the spectroscopic properties of an *open* system are considered. In Sect. 3, the results are given and in Sect. 4, they are discussed. Conclusions are drawn in the last section.

2 Model

The model used in the present calculations is the continuum shell model [3].

The Schrödinger equation

$$(H - E)\Psi = 0 \tag{1}$$

is solved with the ansatz

$$\Psi = \sum_i d_i \Phi_i^{(0)} + \sum_c \int dE' d_c^{E'} \chi_c^{E'} \,. \tag{2}$$

Here, $H = H_0 + V$ is the Hamiltonian of the system with the residual interaction V, the $\Phi_i^{(0)}$ are wavefunctions (Slater determinants) of the unperturbed

discrete states with all A particles in bound states, while the χ_c^E are unperturbed channel wavefunctions with $A-1$ particles in discrete many-particle states and 1 particle in a scattering state.

The spectroscopic values are the widths Γ_R and positions E_R of the resonance states. They follow from

$$(H_{QQ}^{eff} - \tilde{\mathcal{E}}_R)\,\tilde{\Phi}_R = 0 \tag{3}$$

where the $\tilde{\Phi}_R$ are the complex energy dependent eigenfunctions and

$$\tilde{\mathcal{E}}_R = \tilde{E}_R - \frac{i}{2}\tilde{\Gamma}_R \tag{4}$$

are the complex energy dependent eigenvalues of the effective Hamiltonian

$$H_{QQ}^{eff} = QH\,(Q + G_P^{(+)}\,PHQ\,) \tag{5}$$

in the subspace of bound states. Then, the equations

$$E_R = \tilde{E}_R(E = E_R) \tag{6}$$
$$\Gamma_R = \tilde{\Gamma}_R(E = E_R) \tag{7}$$

have to be solved in order to determine the spectroscopic values.

In (5), $G_P^{(+)}$ is the Green function for the motion of the particle in the continuum. Further, Q projects onto the subspace of bound states,

$$Q = \sum_R |\Phi_R^{SM} >< \Phi_R^{SM}|\,, \tag{8}$$

and P onto the environment (subspace of decay channels) with the completeness relation

$$P + Q = 1\,. \tag{9}$$

The bound states Φ_R^{SM} are identified with the solutions of the standard shell model problem, i.e. the Q operator projects onto the shell model function space. In the full Hilbert space $P+Q$, the shell model equation reads

$$\begin{aligned}(H - E_R^{SM})\Phi_R^{SM} &= PHQ\;\Phi_R^{SM} \\ &= (1-Q)\;HQ\;\Phi_R^{SM}\,.\end{aligned} \tag{10}$$

With the total Hamiltonian H, eq. (3) reads

$$(H - \tilde{\mathcal{E}}_R)\,\tilde{\Phi}_R = X\,\tilde{\Phi}_R \tag{11}$$

where

$$X = \left\{1 - QHP\ \left(E^+ - PHP\right)^{-1}\right\} PHQ$$
$$= \left\{1 - QH(1-Q)\left(E^+ - (1-Q)H(1-Q)\right)^{-1}\right\}(1-Q)HQ\ . \quad (12)$$

Eqs. (10), (11) and (12) show clearly that a system being in a subspace of the whole function space is described, in any case, by a Schrödinger equation which is nonlinear with respect to the wavefunctions: Only for $Q = 1$, i.e. for a closed system, eqs. (10) and (11) turn into linear (identical) equations. The unitarity condition is fulfilled due to (9).

The wavefunctions Φ_R^{SM} contain the internal mixing

$$W_{RR'}^{in} = < \Phi_R^{(0)} | V^{in} | \Phi_{R'}^{(0)} > \quad (13)$$

of two states while the wavefunctions $\tilde{\Phi}_R$ contain additionally the external mixing

$$W_{RR'}^{ex} = \sum_c \int dE' < \Phi_R^{SM} | V^{ex} | \xi_{E'}^{c(+)} > \frac{1}{E^{(+)} - E'} < \xi_{E'}^{c(+)} | V^{ex} | \Phi_{R'}^{SM} > \quad (14)$$

of the two states R and R' via the continuum of decay channels. Here, $V^{in} = \alpha^{in} \cdot V$ and $V^{ex} = \alpha^{ex} \cdot V$ where the parameters α^{in} and α^{ex} are introduced in order to vary the internal and external mixing independently of each other. The ξ_E^c are solutions of the coupled channels equations

$$(H - E^{(+)}) \xi_E^{c(+)} = QHP\ \xi_E^{c(+)}\ . \quad (15)$$

The channels c are the so-called physical channels, i.e. the unperturbed channel wavefunctions χ_E^c denote the wavefunction of a nucleon in relative motion to the residual nucleus which is in a definite (discrete) state with definite quantum numbers.

The wavefunction of a resonance state is

$$\tilde{\Omega}_R = \left(Q + G_P^{(+)}\ HQ\right) \tilde{\Phi}_R$$
$$\equiv \tilde{\Phi}_R + \tilde{\omega}_R\ . \quad (16)$$

Here, $\tilde{\omega}_R$ describes the tail of the wavefunction due to the coupling of the state to the continuum. It is

$$< \Omega_R | V | \chi_E^c > = < \Phi_R^{SM} | V | \xi_E^c >\ , \quad (17)$$

where

$$\Omega_R \;=\; (Q + G_P^{(+)}\, HQ)\, \Phi_R^{SM}\,, \tag{18}$$

in analogy to eq. (16), and

$$< \tilde{\Omega}_R|V|\chi_E^c >=< \tilde{\Phi}_R|V|\xi_E^c > \;. \tag{19}$$

The $< \tilde{\Omega}_R|V|\chi_E^c >$ are the amplitudes of the partial widths $\tilde{\gamma}_R^c$ while the $< \Phi_R^{SM}|V|\xi_E^c >$ are the coupling matrix elements between discrete and scattering states. The values $< \tilde{\Omega}_R|V|\chi_E^c >$ may differ strongly from each other even for states with the same total quantum numbers whereas the $< \Phi_R^{SM}|V|\xi_E^c >$ are of the same order of magnitude for different states R.

It is

$$\sum_R \tilde{\Gamma}_R(W_{RR'}^{ex}) = const \tag{20}$$

at every energy E of the system and constant diagonal matrix elements W_{RR}^{ex}. Such a case occurs, e.g., if the level density is enlarged, in the numerical calculations, by reducing the level distances [7]. Eq. (20) is nothing but the fact that the sum of the eigenvalues of a matrix is equal to the sum of the diagonal matrix elements [3]. It expresses the condition under which the external mixing $W_{RR'}^{ex}$ of the resonance states of the system takes place.

If one considers the behaviour of the system as a function of the coupling strength $V = V^{ex}$ in (14), then the right-hand side of eq. (20) is a monotonously increasing function of V^{ex}, since the N diagonal matrix elements W_{RR}^{ex} depend monotonously on V^{ex}. Nevertheless, a redistribution can be achieved, also in this case, by the $N(N-1)$ nondiagonal matrix elements $W_{RR'}^{ex}$.

In any case, the redistribution taking place at high level density occurs in accordance with the unitarity of the S-matrix. The resonance part of the S-matrix reads [3]

$$S_{cc'}^{(2)} = i \sum_R \frac{\tilde{\gamma}_{Rc'}^{1/2}\; \tilde{\gamma}_{Rc}^{1/2}}{E - \tilde{E}_R + \frac{i}{2}\tilde{\Gamma}_R}\,. \tag{21}$$

Let us consider an ensemble of N resonances which lie densely in an energy region ΔE comparable to the uncertainty of energy of the system ($E \approx E_1 \approx E_2 ... \approx E_N$). Due to external mixing, they interfere strongly and one gets for estimation

$$S_{cc'}^{(2)} \approx 2 \sum_R \frac{\tilde{\gamma}_{Rc'}^{1/2}\; \tilde{\gamma}_{Rc}^{1/2}}{\tilde{\Gamma}_R}\,. \tag{22}$$

In the one-channel case, it is

$$S_{cc}^{(2)} \approx 2 \sum_{R_f} \frac{\tilde{\gamma}_{R_f c}}{\tilde{\gamma}_{R_f c}} \tag{23}$$

where the R_f denote the relevant fast modes and the relation

$$\tilde{\Gamma}_R = \sum_c |\tilde{\gamma}_{Rc}| \tag{24}$$

for these modes has been used (see *Fig. 4* and the corresponding discussion). According to the unitarity of the S-matrix, $|S_{cc}^{(2)}| \leq 2$. Therefore, the number R_f of relevant fast modes cannot be larger than 1 in the case with one open decay channel. An analogous conclusion can be drawn in the many-channel case: The number of fast relevant modes is exactly equal to the number K of open decay channels.

As a result, the widths of K states increase up to their maximal possible value at the cost of the widths of the remaining $N - K$ ones where N is the number of states and K the number of open decay channels,

$$\sum_{R=1}^{K} \tilde{\Gamma}_R(W^{ex}) \approx \sum_{R=1}^{N} \tilde{\Gamma}_R(W^{ex}) \tag{25}$$

and

$$\sum_{R=K+1}^{N} \tilde{\Gamma}_R(W^{ex}) \approx 0 \, . \tag{26}$$

The $N - K$ states with small widths, according to (26), are called trapped modes [3].

It could be shown analytically [2, 16] that at high level density where the resonance states overlap, the relation (24) between total widths and partial widths does no longer hold. Instead, it is proven

$$\tilde{\Gamma}_R \; < \tilde{\Phi}_R | \tilde{\Phi}_R > = \sum_c |\tilde{\gamma}_{Rc}| \, , \tag{27}$$

i.e.

$$\tilde{\Gamma}_R \leq \sum_c |\tilde{\gamma}_{Rc}| \tag{28}$$

at high level density. The relation (28) holds also for the one-channel case when the states are mixed via one continuum. Eq. (24) holds only for isolated resonance states.

3 Calculations and Results

The calculations are performed for 70 states with $J^\pi = 1^-$ in ^{16}O with (1p-1h) and (2p-2h) excitations. The configurational space is $(1p)^{-1}(2s, 1d_{5/2})^1$, $(1s)^{-1}(1p)^{-1}(2s, 1d_{5/2})^2$. The parameters of the Woods-Saxon potential are similar to those used in realistic calculations, see e.g. [17]. The residual interaction is a zero-range force

$$V(1,2) = -\alpha V_0(a + bP^\sigma_{12})\delta(\mathbf{r}_1 - \mathbf{r}_2) \,, \tag{29}$$

where P^σ_{12} is the spin exchange operator and α is a parameter which controls the coupling strength between bound ($\alpha = \alpha^{in}$) as well as between bound and unbound ($\alpha = \alpha^{ex}$) states.

In our calculations, we use $V_0 = 500MeV \cdot fm^3$, $a = 0.73$, $b = 0.27$ which are realistic values for ^{16}O (see [17], where $V_0 = 650MeV \cdot fm^3$). The energy of the system (energy of the projectile) was fixed mostly at $E_{cm} = 34.7$ MeV. Calculations at other energies are performed, but not shown in the present paper, because they lead qualitatively to the same results. Most of the 70 states lie in an energy region of E_{cm} between about 25 MeV to 45 MeV.

The number of channels taken into account in our calculations is two. They correspond to $^{15}N + p$ with ^{15}N in its ground and first excited state at 6.3 MeV with negative parity ($1h$-structure).

The calculations are performed as a function of the "control" (coupling) parameter α^{ex} which controls the value of the coupling matrix elements between bound and scattering states (external coupling parameter α^{ex} in (14)). It is varied independently from the parameter α^{in} in the matrix elements between bound states (internal coupling parameter α^{in} in (13)) which is fixed in our calculations to $\alpha^{in} = 1$. It should be underlined that the parameter α^{in} appears linearly in the internal mixing W^{in}, (13), while the relation between α^{ex} and W^{ex} is more complicated: Additionally to the explicit quadratic dependence on α^{ex}, the W^{ex} depend on α^{ex} via the coupled channel wavefunctions ξ^c_E, eq. (15).

In order to illustrate the trapping effect, the imaginary parts $\frac{1}{2}\tilde{\Gamma}_R$ of the complex eigenvalues of the effective Hamiltonian H^{eff}_{QQ} are calculated as a function of the coupling strength V^{ex} in the case of two open decay channels and shown in *Fig. 1.* As long as α^{ex} is small, the widths of all modes increase with increasing coupling strength V^{ex} between bound and continuous states. Beyond some critical value α^{ex}_{cr}, the widths of most trapped modes *decrease* with increasing coupling strength while in some cases they *increase very slowly.* In contrast to this, the widths of the broad modes *increase very*

quickly with increasing coupling strength V^{ex} from the very beginning. As a result, the widths of the trapped modes are much smaller than those of the two fast modes for $\alpha > \alpha_{cr}$.

The growing-up of the two short-lived modes is shown in *Fig. 2*. Here, the widths of the resonances are drawn for different coupling parameters α^{ex} reaching from 1 to 9. The resonances are sorted along the x-axis according to the value of their width: the first resonance has the largest width Γ_1 while the 70th resonance has the smallest width Γ_{70}. In *Fig. 2*, the widths of the first 20 resonances are shown. The separation of the two broad resonances occurs at $\alpha_{cr}^{ex} \approx 2.5$ to 3.

According to relation (27), the total width $\tilde{\Gamma}_R$ of a state differs from the sum of the partial widths $|\tilde{\gamma}_R^c|$ by the factor $< \tilde{\Phi}_R | \tilde{\Phi}_R >$. In *Fig. 3*, $< \tilde{\Phi}_R | \tilde{\Phi}_R >$ is given for all 70 resonances and different α^{ex}. As one can see from the figure, $< \tilde{\Phi}_R | \tilde{\Phi}_R >$ stays always below 3 with the exception of a few comparably narrow regions of α^{ex} where further redistributions in the system take place. The total widths $\tilde{\Gamma}_R$ of the broad and trapped modes differ, on the average, by several orders of magnitude at a large coupling strength α^{ex}. As a consequence, the partial widths of the broad and trapped modes differ strongly, too.

In *Fig. 4*, the dependence of $< \tilde{\Phi}_R | \tilde{\Phi}_R >$ on α^{ex} is shown for the two fast (f) modes (*Fig. 4a*) as well as for some slow (s) modes (*Fig. 4b,c*). For the fast (broad) modes, the scalar product increases up to 6 in the critical region where the redistribution in the nucleus occurs. For larger α^{ex}, it decreases again. Below and beyond the critical region, $< \tilde{\Phi}_R^f | \tilde{\Phi}_R^f > \approx 1$, i.e. the resonances R_f behave like usual resonances in the sense of relation (24). This result corresponds to the conclusion drawn e.g. in [5], that the fast modes are relevant. Further, the estimation (23), where (24) has been used, is justified.

The wavefunctions $\tilde{\Phi}_R^s$ of the other modes show a different behaviour (*Fig. 4*). For most of them, $< \tilde{\Phi}_R^s | \tilde{\Phi}_R^s >$ remains larger 1 for large α^{ex}. The "gaps" in *Figs. 4b, c* arise because the ordering of the resonances according to the value of their widths changes with α^{ex}.

In *Fig. 5*, the widths $\tilde{\Gamma}_R$ are shown as a function of the energy E_{cm} of the system for $\alpha^{ex} = 2$ and 6. The position of the inelastic threshold is at $E_{cm} = 6.3$ MeV (*Fig. 5a,b*) and shifted to 30.0 MeV (*Fig. 5c,d*). The $\tilde{\Gamma}_R^f$ depend smoothly on energy with the exception of threshold effects. The influence of the inelastic threshold on the widths can be seen at all α^{ex} (*Fig. 5c,d*). The pictures show clearly the appearance of one broad mode below the inelastic threshold at large α^{ex}, while there are two broad modes as soon

as two channels are open. It is interesting to see that the one broad mode below the inelastic threshold is not among the two broad modes above the threshold. This result illustrates very nicely that the original spectroscopic information of a state is not decisive for the question whether a mode becomes trapped or relevant.

The average degree of overlapping $\bar{\Gamma}/\bar{D}$ of the resonances as a function of the coupling parameter α^{ex} is shown in *Fig. 6.* The degree of overlapping of the two broad modes increases strongly in the region of the instability point and decreases at larger α^{ex} where the two resonances repel each other. The degree of overlapping of the trapped modes is almost constant or decreases in the region of the instability point while it increases weakly for higher values α^{ex} even if the four broadest trapped modes are excluded ("64s").

The complex eigenvalues $\tilde{E}_R - \frac{i}{2}\tilde{\Gamma}_R$ of the Hamiltonian H^{eff}_{QQ} (eqs. (3) and (5)) are shown in *Figs. 7 and 8* as a function of the coupling parameter α^{ex}. Starting from the value $\alpha^{ex}_{min} = 0.05$, the parameter α^{ex} is changed in steps of 0.05 up to $\alpha^{ex}_{max} = 1$ (*Fig. 8a*), 2 (*Fig. 8b*), ... , 8 (*Fig. 8g*) and 9.8 (*Fig. 7*). At $\alpha^{ex}_{cr} \approx 2.6$, two broad modes are formed. After leaving the energy region where the narrow 68 resonance states remain, new generations of "broad" modes appear: At $\alpha^{ex} = 4.5$, 6.5 and 9, relatively broad modes at both the lower-energy and the higher-energy parts of the spectrum are growing on. The corresponding redistributions in the nuclear system can be seen in *Fig. 3.* It is interesting to observe that the widths of some trapped modes decrease for relatively small α^{ex} but increase again for larger α^{ex}. This shows once more that the original spectroscopic information contained in the shell model wavefunctions Φ^{SM}_R of the discrete states is lost and is not decisive for the lifetime of a special state after the redistribution has taken place.

4 Discussion of the results

The results obtained for the open nuclear quantum system as a function of the control parameter α^{ex} are represented in *Figs. 1 to 8.* It exists a critical value α^{ex}_{cr} of the coupling parameter at which a redistribution inside the nucleus takes place. The two corresponding scenarios $\alpha^{ex} < \alpha^{ex}_{cr}$, corresponding to a low level density, and $\alpha^{ex} > \alpha^{ex}_{cr}$, corresponding to a high level density, are very well known in nuclear physics. For their description, phenomenological models have been worked out: At low level density, the discrete states where all nucleons occupy bound single-particle states are relevant, while at higher level density the coupled channels are relevant ("unified theory of nuclear reactions" [18]). This picture corresponds exactly to the results ob-

tained by us. The transition we observe at the critical coupling parameter α_{cr}^{ex} occurs from a scenario with N relevant discrete states to another one in which the K open decay channels are relevant [3].

Furthermore, the results obtained numerically in this paper, agree fully with the behaviour of selforganizing systems studied on the basis of *classical* methods by Haken et al. [4] although the system investigated by us is described as an open *quantum* system. At the transition, a few unstable (short-lived) states are formed, in both cases, together with many stable (long-lived) states. The unstable modes are relevant (see for illustration [5] where the S-matrix is studied for a quantum system as a function of the level density). Thus, the trapping process reduces the effective number of degrees of freedom and the complexity of the system, respectively, as expected for a selforganizing system. The number of different decay possibilities decreases with increasing coupling strength.

The analogy of our results with those obtained by Haken [4] consists in the following.

The behaviour of the system is investigated in both cases in dependence on a *control parameter*. In the nuclear system, this parameter is α^{ex} which characterizes the coupling strength between system and environment of decay channels.

Most interesting is the behaviour of the system near to an *instability point* since here a rearrangement takes place inside the system which is very sensitive to the control parameter. The instability point in the nuclear system corresponds to α_{cr}^{ex}, where the resonances start to overlap, more exactly where the average distance $\bar{D}$ between the resonances is equal to their average width $\bar{\Gamma}$. Here, the nuclear system has the possibility to form a few short-lived modes together with trapped modes most of which decouple practically from the environment.

The behaviour of resonances at the instability point $\bar{\Gamma}/\bar{D}$ has been investigated in an earlier paper [14] on the basis of the statistical theory of nuclear reactions in which not only the internal mixing of the resonance states is not taken into account but also the energy dependence of the coupling matrix elements between discrete and continuous states is neglected. In these investigations, the widths of *all* trapped modes decrease with increasing coupling strength α^{ex}. There are no broad modes of the second and third generation in contrast to the results obtained in the present investigations. Furthermore, the energy shifts of the trapped modes in the calculations of the statistical model are of such a type that the energy region covered by the whole group of

resonances is reduced. In the present more realistic calculations, the results are much more multiform. A nice example for the great variety of the results in a more realistic model is the appearance of a new fast mode at the energy where a new decay channel opens (*Fig. 5*). In an analogous manner, local broad modes of the second or third generation appear as soon as the two fast modes are shifted to an energy outside the main interference region (*Fig. 8*).

In the strong-coupling regime, the trapped modes are almost decoupled from the environment of decay channels: The coupling matrix elements (17) are large but the matrix elements (19), which correspond to the amplitudes of the partial widths, are extremely small (see *Figs. 1, 2, 5, 7 and 8*). This result corresponds fully to the definition of the compound nucleus given by N. Bohr more than 50 years ago [19]. He claimed: "In the atom and in the nucleus we have indeed to do with two extreme cases of mechanical many-body problems for which a procedure of approximation resting on a combination of one-body problems, so effective in the former case, loses any validity in the latter where we, from the very beginning, have to do with essential collective aspects of the interplay between the constituent particles."

The *"order parameters"* [4] may be identified with the wavefunctions of the broad modes. It follows from eq. (16)

$$\tilde{\Omega}_R = \tilde{\Phi}_R + \sum_c \int_{\epsilon_c} dE' \, \frac{1}{E - E'} \, \xi_E^c \; < \xi_E^c | V | \tilde{\Phi}_R > \tag{30}$$

and further by using eq. (27),

$$\tilde{\Omega}_R \approx \tilde{\Phi}_R + i\pi \; e^{i\delta_c} \; \xi_E^c \; \Gamma_R^{1/2} \; < \tilde{\Phi}_R | \tilde{\Phi}_R >^{1/2} \tag{31}$$

in the one-channel case. From (31), it follows

$$\frac{< \xi_E^c | \tilde{\Omega}_R^f >}{< \xi_E^c | \tilde{\Omega}_R^s >} \approx \left(\frac{\Gamma_R^f}{\Gamma_R^s} \right)^{1/2} \tag{32}$$

by using the numerical results shown in *Fig. 3*. As a result, the wavefunctions of the broad modes overlap strongly with the channel wavefunctions due to the large contribution $\tilde{\omega}_R^f$ in $\tilde{\Omega}_R^f$. The wavefunctions of the trapped modes, on the contrary, are described well by the $\tilde{\Phi}_R$,

$$\tilde{\Omega}_R^s \approx \tilde{\Phi}_R^s \, . \tag{33}$$

Further, the fast modes behave like isolated resonances (see below) although they *do* overlap (*Fig. 6*). This result is surely connected with the fact that the channel wavefunctions $\{\xi_E^c\}$ for different channels c are orthogonal to

each other. Therefore, the large overlapping integrals $< \xi^c_E|\tilde{\Omega}^f_R >$ suggest $< \tilde{\Omega}^f_R|\tilde{\Omega}^f_{R'} > \approx \delta_{RR'}$.

Thus, it is justified to identify the trapped modes with the stable enslaved modes and the broad modes with the enslaving unstable modes. The *slaving principle* is illustrated directly in *Fig. 4*: The unstable modes behave like isolated resonances with the exception of the region around α^{ex}_{cr}, at which the rearrangement inside the nucleus takes place (*Fig. 4a*) and where their wavefunctions are complex. At higher coupling strength, the two resonances repel each other. That means, they are described quite well by neglecting the trapped modes altogether.

The trapped modes are almost stable. Near to the instability point, their average degree $\bar{\Gamma}/\bar{D}$ of overlapping is almost constant or decreases due to their small widths (*Fig. 6*). For larger α^{ex}, it increases slowly with increasing coupling strength what is connected with the appearance of broad modes of the second and third generation (compare *Figs. 7, 8*). The trapped modes do not behave like isolated resonances neither in the region where $\bar{\Gamma}/\bar{D}$ is almost constant, as can be seen from *Fig. 4b,c*, nor in the region where the "broad" modes of the second and third generation appear. All of them are "enslaved" by the two fast modes by which they are overlapped. By this, the influence of the unstable modes on the stable ones is expressed ("slaving principle").

In [14], it is shown, basing on results obtained in the statistical model, that trapping of resonance states and enveloping them by broad modes occurs as soon as the local level density is high enough so that some resonance states overlap due to *local* fluctuations in the level density. The trapping appears for a small localized group of resonances, in those calculations, in the same manner as for large extended groups. That means, the trapping mechanism proceeds in a *hierarchical* way. In the present calculations, we observe also a hierarchical mechanism of trapping (*Figs. 7, 8*). The wavefunctions of the local broad modes, however, differ from the fast modes of the system since they do not behave like isolated resonances (*Fig. 4*). They are, on the one hand, slaved by the modes of the higher hierarchies and, on the other hand, slave locally trapped states.

The picture obtained from the present realistic calculations is richer in the sense that a second and a third "generation" of broad modes at higher α^{ex} appear (*Figs. 7, 8*). These resonances do not behave like isolated resonances (see *Fig. 4b*). Inspite of their increasing widths as a function of the coupling parameter α^{ex}, they do not have the order properties of the two first broad modes appearing at $\alpha^{ex}_{cr} \approx 2.6$. They are of local importance and

create local "bumps" among the finestructure resonances.

The *relevance of the unstable modes* at time and energy scales characteristic of the system is discussed in earlier papers (e.g. [3, 5]). By means of these modes, the system finds its own structure. The *stable (trapped)* modes can be identified in the cross section only at the long-time scale which is *not typical* for the system considered. The properties of the trapped modes are *generic*, see e.g. [11].

The physical meaning of this result is the following: the rearrangement inside the nucleus, taking place at the critical coupling strength V_{cr}^{ex}, occurs in such a manner that the *complexity* of the system is *reduced.* Due to trapping, many degrees of freedom become irrelevant. In other words: By reducing the number of relevant degrees of freedom, the system finds its own structure with an energy and time scale characteristic of it.

It should be underlined here, that the results discussed in the present paper are obtained for an open *quantum* system described by a *nonlinear* Schrödinger equation. The mathematical formalism used here coincides fully with the standard methods worked out for the description of the nucleus in the two limiting cases at low and at high level density. In these limiting cases, the nonlinearity of the Schrödinger equation can be neglected since one restricts oneself, in the standard methods, to the description of the relevant modes.

In spite of the difference in the mathematical formalism used in this paper and in other investigations of selforganizing systems, the results obtained by us coincide with those from synergetics. In any case, the system redistributes at a certain critical value of the control parameter in such a manner that the effective number of degrees of freedom is reduced.

5 Summary

In the present paper, the rearrangement is investigated in detail which takes place in the nuclear system if the level density is so large that the distance between the resonances is comparable with their widths, on the average. The rearrangement proceeds in such a manner that the spectroscopic information on the resonance states which is relevant at low level density is lost at high level density. Instead, a few unstable modes become relevant the number of which is exactly equal to the number of open decay channels. These two scenarios are very well known in nuclear physics. For the description of their

respective relevant parts, phenomenological methods have been worked out.

The transition between the two scenarios is traced by us as a function of a control parameter which describes the coupling of the discrete states of the system to the environment of decay channels. The model used is the continuum shell model which describes the nucleus as an open quantum mechanical system. It is a realistic model for light nuclei.

As a result, the transition takes place in full analogy to transitions in other selforganizing systems which are described by classical methods. By means of numerical results, the *slaving principle of synergetics* is shown to hold also for the nuclear system.

The experimental observation of structures in the nuclear reaction cross sections even at high level density was always surprisingly in the history of nuclear physics studies. According to the numerical results obtained by us, they are caused by unstable modes formed locally at high level density. These states slave some trapped modes ("fine structure resonances").

In spite of their small widths, the trapped modes do *not* behave like isolated resonances which are independent from each other. They are correlated due to the existence of the broad unstable modes by which they are overlapped. It is worth-while to mention that such a result follows not only from the numerical calculations given in this paper but is very well known from experimental nuclear physics studies, e.g. from the isobaric analogue resonances. Phenomenological models have been worked out for their description [2]. Furthermore, correlations are found recently between neutron resonances [20, 21, 22]: The parity violation measured in resonant neutron reactions shows strong sign correlations which are *not* a feature of the conventional statistical model of parity mixing between compound nucleus states.

Summarizing, we have shown in this paper by means of numerical results, that the slaving principle of synergetics holds also in the *open quantum mechanical* nuclear system. In a forthcoming paper, the principle of maximum information entropy will be studied for the nuclear system in the framework of the same model.

Acknowledgment: The present investigations are supported by the Deutsche Forschungsgemeinschaft (Ro 922/1) and by the Bundesministerium für Forschung und Technologie (WTZ X081.39).

References

[1] A. Bohr and B.R. Mottelson, *Nuclear Structure* (London: Benjamin) 1975

[2] C. Mahaux and H.A. Weidenmüller, *Shell-Model Approach to Nuclear Reactions* (Amsterdam: North-Holland) 1969

[3] I. Rotter, Rep. Progr. Phys. 54, 635 (1991) and references therein

[4] H. Haken, *Advanced Synergetics* (Berlin, Heidelberg: Springer) 1987; *Information and Selforganization* (Berlin, Heidelberg: Springer) 1988

[5] F.M. Dittes, W. Cassing and I. Rotter, Z. Phys. A 337, 243 (1990)

[6] V.V. Sokolov and V.G. Zelevinsky, Phys. Lett. B 202, 10 (1988); Nucl. Phys. A 504, 562 (1989)

[7] P. Kleinwächter and I. Rotter, Phys. Rev. C 32, 1742 (1985)

[8] V.B. Pavlov-Verevkin, Phys. Lett. A 129, 168 (1988);
F. Remacle, M. Munster, V.B. Pavlov-Verevkin and M. Desouter-Lecomte, Phys. Lett. A 145, 265 (1990)

[9] I. Rotter, J. Phys. G12, 1407 (1986) and G 14, 857 (1988); Fortschr. Phys. 36, 781 (1988)

[10] F.M. Dittes, H.L. Harney and I. Rotter, Phys. Lett. A 153, 451 (1991)

[11] F.M. Dittes, I. Rotter and T.H. Seligman, Phys. Lett. A 158, 14 (1991)

[12] V.V. Sokolov and V.G. Zelevinsky, Ann. Phys. (N.Y.) 216, 323 (1992)

[13] F. Haake, F. Izrailev, N. Lehmann, D. Saher, and H.J. Sommers, Z. Phys. B 88, 359 (1992)

[14] W. Iskra, I. Rotter and F.M. Dittes, Preprint FZR 92 - 05 (Rossendorf 1992); Phys. Rev. C (in press)

[15] H.S. Taylor, International Journal of Quantum Chemistry 31, 747 (1987)

[16] I. Rotter, J. Phys. G 5, 1575 (1979)

[17] H.W. Barz, I. Rotter and J. Höhn, Nucl. Phys. A 275, 111 (1977)

[18] H. Feshbach, Ann. Phys. (N.Y.) 19, 287 (1962)

[19] N. Bohr, Nature 137, 344 (1936)

[20] J.D. Bowman *et al.*, Phys. Rev. Letters 65, 1192 (1990);
C.M. Frankle *et al.*, Phys. Rev. Letters 67, 564 (1991);
J.D. Bowman *et al.*, Phys. Rev. Letters 68, 780 (1992);
M.B. Johnson *et al.*, Phys. Rev. C 45, 437 (19929

[21] G.E. Mitchell, "From spectroscopic to chaotic features of nuclear systems", Proceedings Symposium Gaussig (Germany), November 1991, World Scientific

[22] H.A. Weidenmüller, "From spectroscopic to chaotic features of nuclear systems", Proceedings Symposium Gaussig (Germany), November 1991, World Scientific

---

Figure 1

The imaginary part of the complex eigenvalues $\tilde{\mathcal{E}}_R = \tilde{E}_R - \frac{i}{2}\tilde{\Gamma}_R$ versus α^{ex}. The calculations are performed at $E = 34.7$ MeV for $\alpha^{in} = 1$, $N = 70$ resonance states and $K = 2$ open decay channels.

Figure 2

The imaginary part $\tilde{\Gamma}_R$ of the complex eigenvalues $\tilde{\mathcal{E}}_R$, multiplied by two, for $\alpha^{ex} = 1, 2, \ldots, 9$ versus the 20 resonance states with the largest widths ($\alpha^{in} = 1$, E=34.7 MeV, N=70, K=2).

Figure 3

The $< \tilde{\Phi}_R | \tilde{\Phi}_R >$ as a function of α^{ex} ($\alpha^{in} = 1$, E=34.7 MeV, N=70, K=2).

Figure 4

The $< \tilde{\Phi}_R | \tilde{\Phi}_R >$ as a function of α^{ex} for the two fast modes (**4a**), the four broadest trapped modes (**4b**) and other trapped modes (**4c**) ($\alpha^{in} = 1$, E=34.7 MeV, N=70, K=2).

Figure 5

The imaginary part $\frac{1}{2}\tilde{\Gamma}_R$ of the complex eigenvalues $\tilde{\mathcal{E}}_R$ versus the center-of-mass energy E of the system ($E_R = E + 12.1MeV$) for $\alpha^{ex} = 2$ (**5a,c**) and 6 (**5b,d**). The second channel opens at 6.3 MeV (**5a,b**) and at 30.0 MeV (**5c,d**), respectively ($\alpha^{in} = 1$, E=34.7 MeV, N=70, K=2).

Figure 6

$\bar{\Gamma}/\bar{D}$ versus α^{ex} for the two broad modes (**f**) and the 68 trapped modes with (**68s**) and without (**64s**) the 4 broadest ones ($\alpha^{in} = 1$, E=34.7 MeV, N=70, K=2).

Figure 7

The complex eigenvalues $\tilde{\mathcal{E}}_R = \tilde{E}_R - Q - \frac{i}{2}\tilde{\Gamma}_R$ for α^{ex} varied from 0.05 up to 9.8 in steps of 0.05. $Q = 12.1$ MeV is the energy of the elastic threshold (Q-value). The results are shown in a logarithmic ordinate scale ($\alpha^{in} = 1$, E=34.7 MeV, N=70, K=2).

Figure 8

The complex eigenvalues $\tilde{\mathcal{E}}_R = \tilde{E}_R - Q - \frac{i}{2}\tilde{\Gamma}_R$ for different α^{ex}. In each picture, α^{ex} is varied from 0.05 to 1 (**8a**), 2 (**8b**), 3 (**8c**), 4 (**8d**), 5 (**8e**), 6 (**8f**), 7 (**8g**), and 8 (**8h**) in steps of 0.05. $Q = 12.1$ MeV is the energy of the elastic threshold (Q-value). The results are shown in a linear ordinate scale ($\alpha^{in} = 1$, E=34.7 MeV, N=70, K=2).

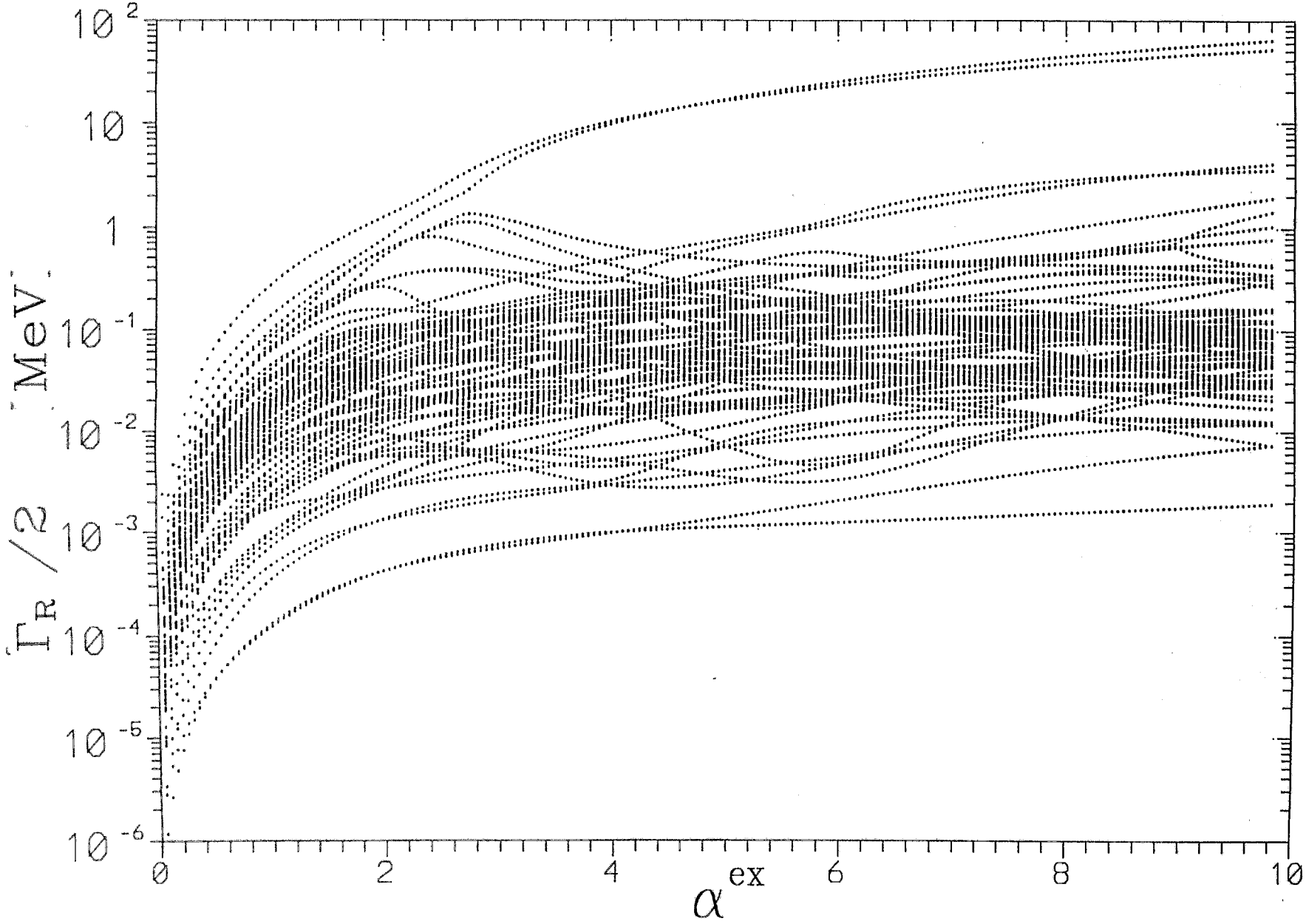
10^{2}
10
1
10^{-1}
10^{-2}
10^{-3}
10^{-4}
10^{-5}
10^{-6}
Γ_R /2 MeV
0
2
4
6
8
10
α^{ex}

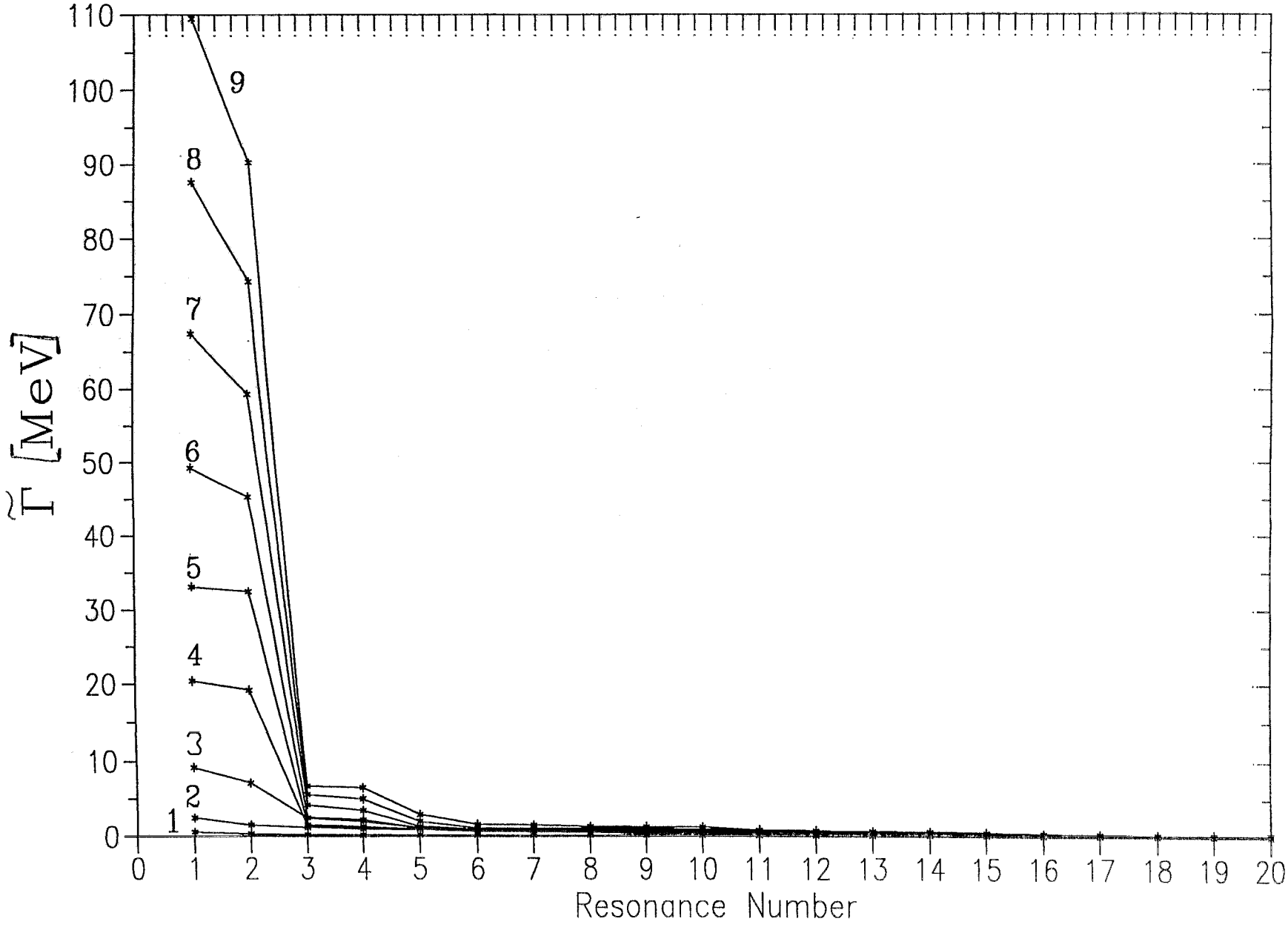
110
100
90
80
70
60
50
40
30
20
10
0
Γ [MeV]
9
8
7
6
5
4
3
2
1
0 1 2 3 4 5 6 7 8 9 10 11 12 13 14 15 16 17 18 19 20
Resonance Number

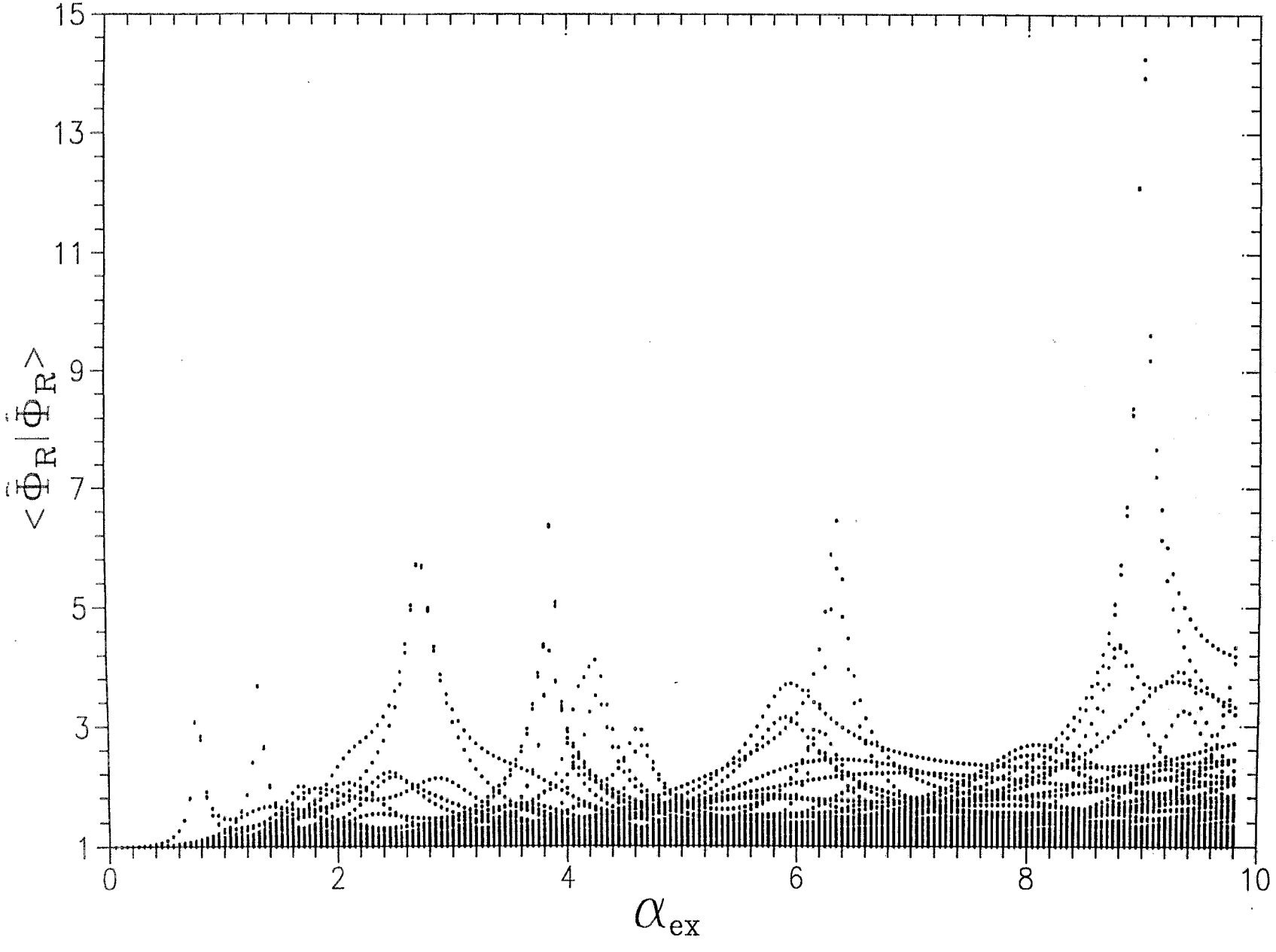
15
13
11
9
7
5
3
1
0
2
4
6
8
10
α_{ex}
$<\tilde{\Phi}_R|\tilde{\Phi}_R>$

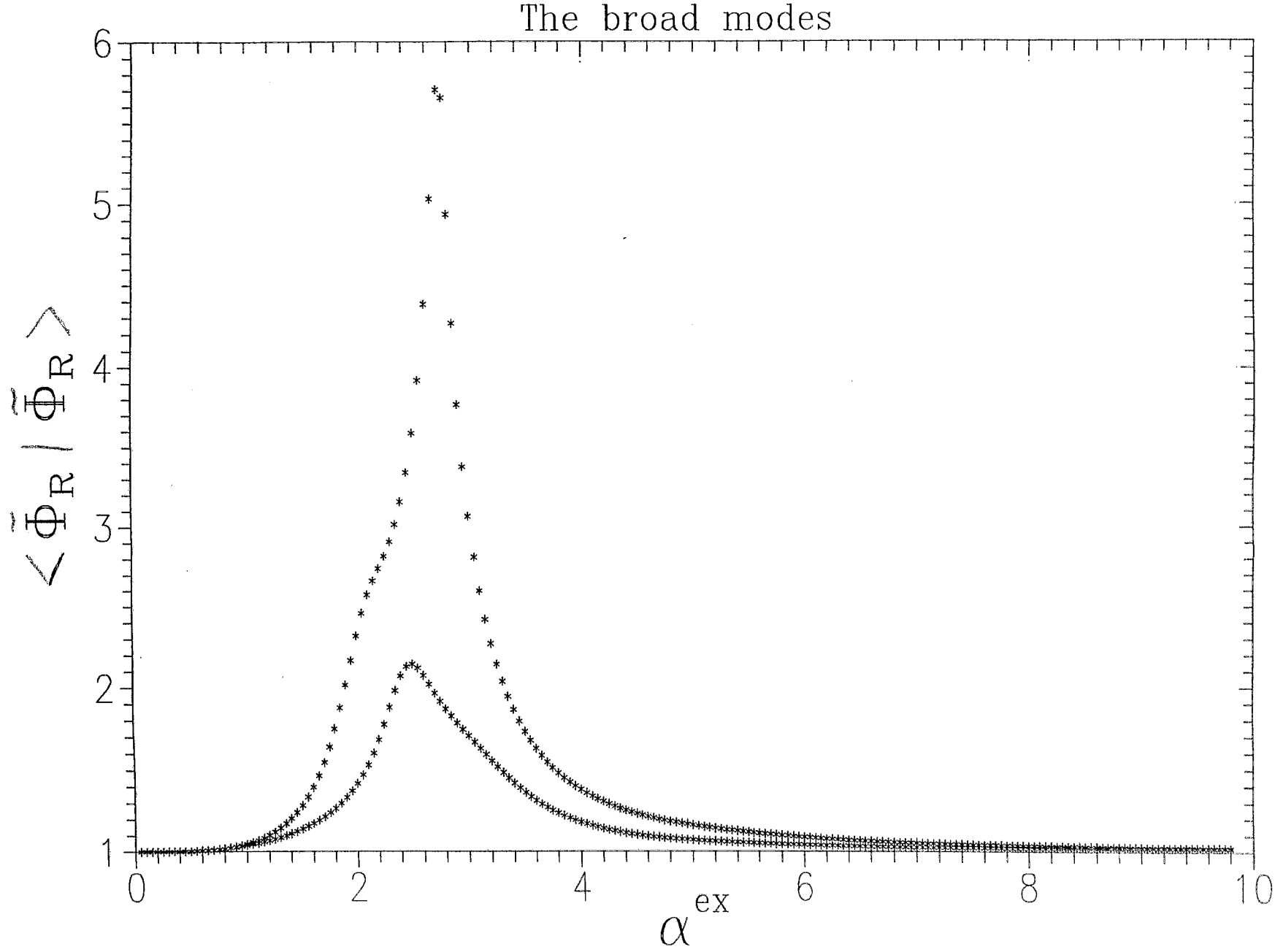
The broad modes
6
5
4
3
2
1
0
2
4
6
8
10
α^{ex}
$\langle \tilde{\Phi}_R | \tilde{\Phi}_R \rangle$

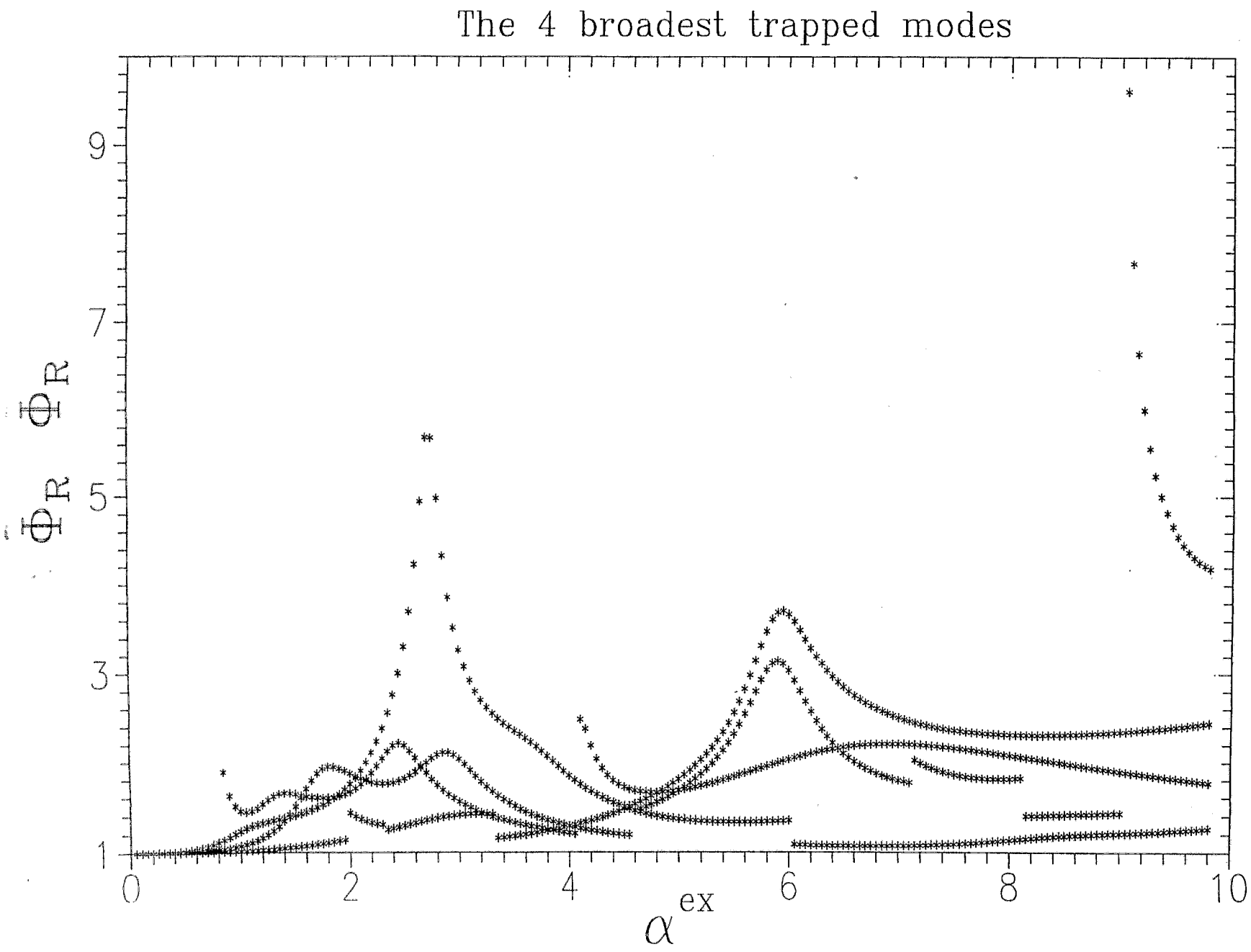
The 4 broadest trapped modes
Φ_R Φ_R
1
3
5
7
9
0
2
4
6
8
10
α^{ex}

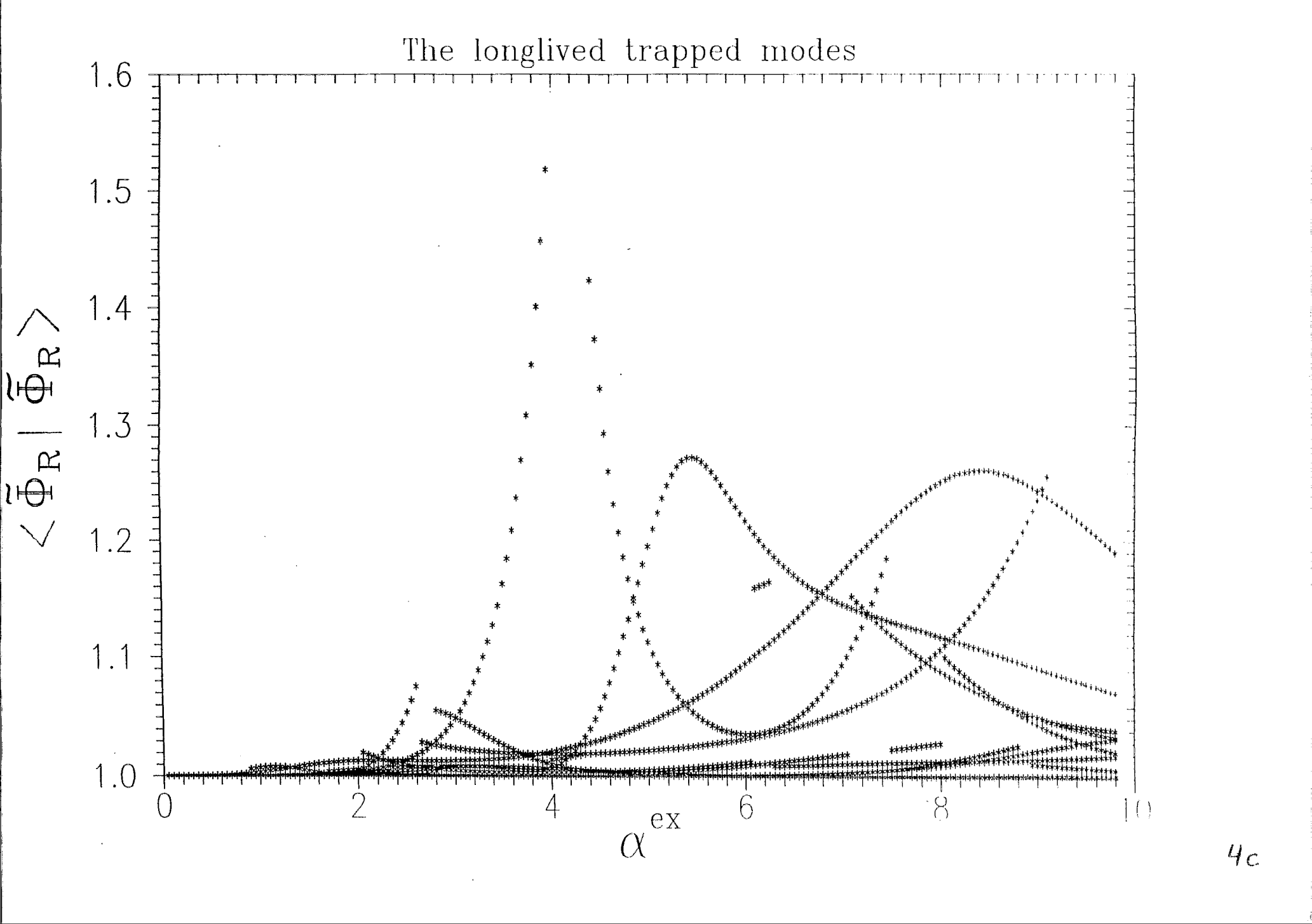
The longlived trapped modes
1.6
1.5
1.4
1.3
1.2
1.1
1.0
0
2
4
6
8
10
α^{ex}
$\langle \tilde{\Phi}_R | \tilde{\Phi}_R \rangle$

4c

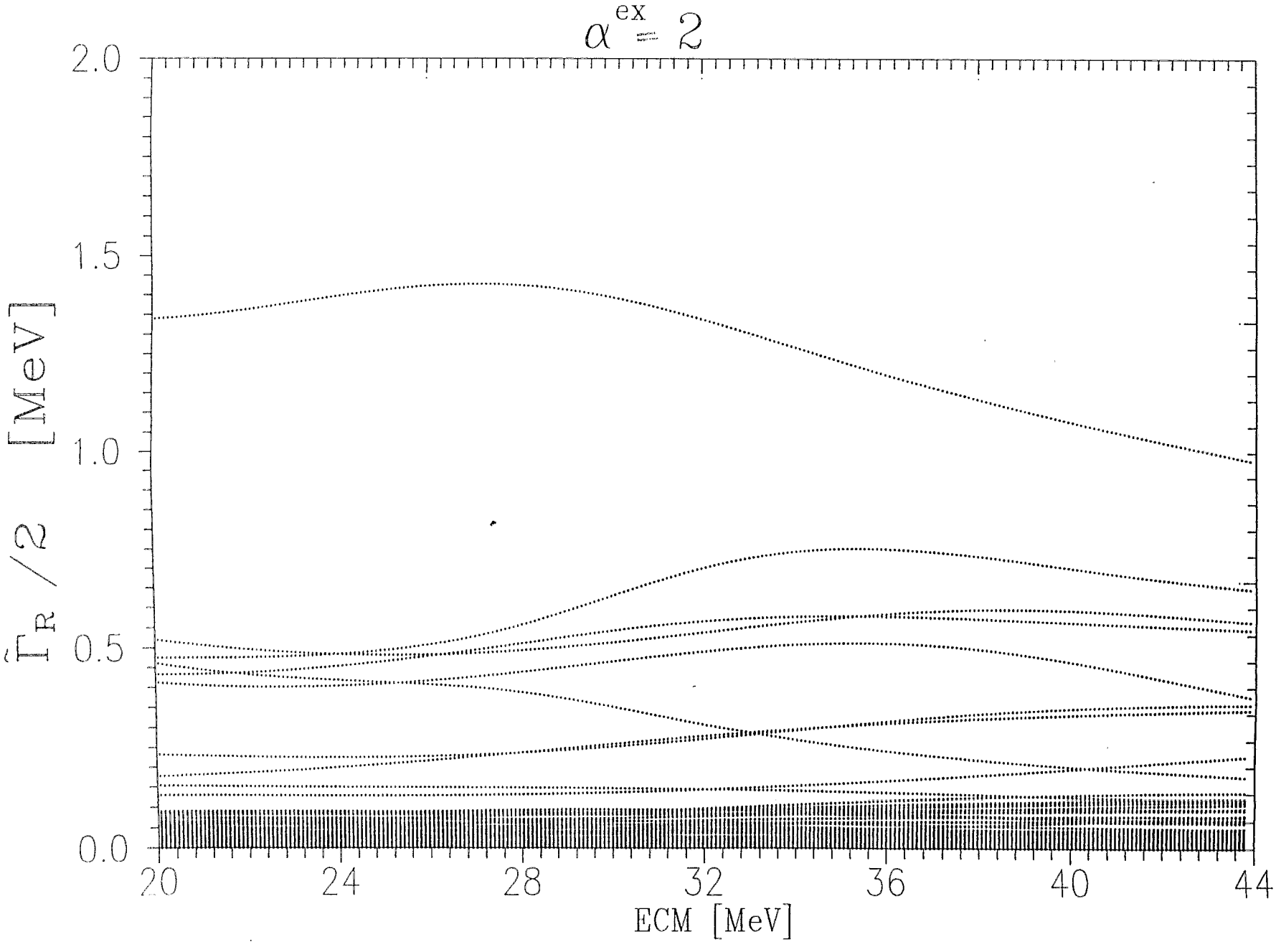
$\alpha^{ex} = 2$
2.0
1.5
1.0
0.5
0.0
$\tilde{\Gamma}_R / 2$ [MeV]
20
24
28
32
36
40
44
ECM [MeV]

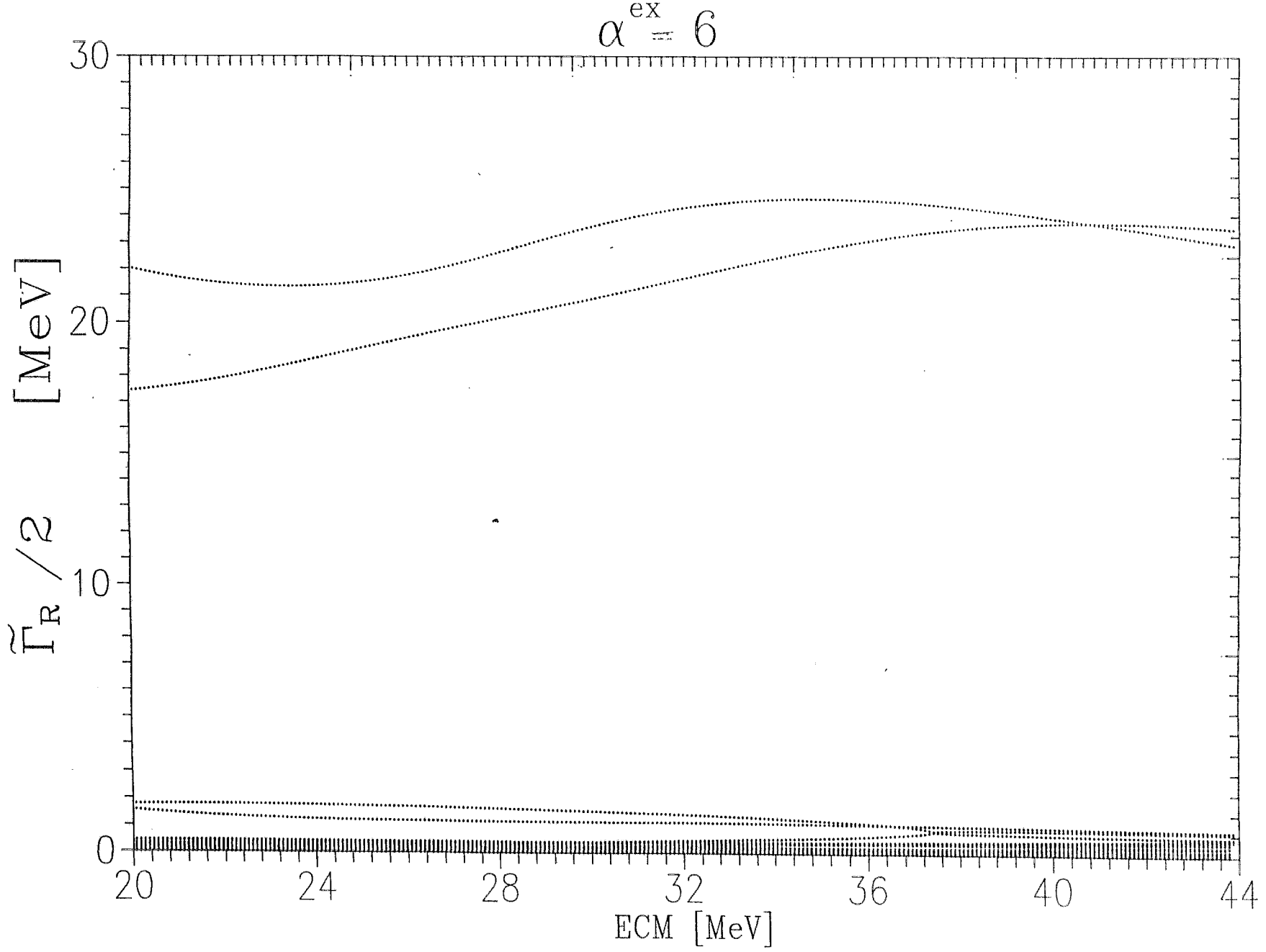
$\alpha^{ex} = 6$
30
20
10
0
$\tilde{\Gamma}_R / 2$ [MeV]
20
24
28
32
36
40
44
ECM [MeV]

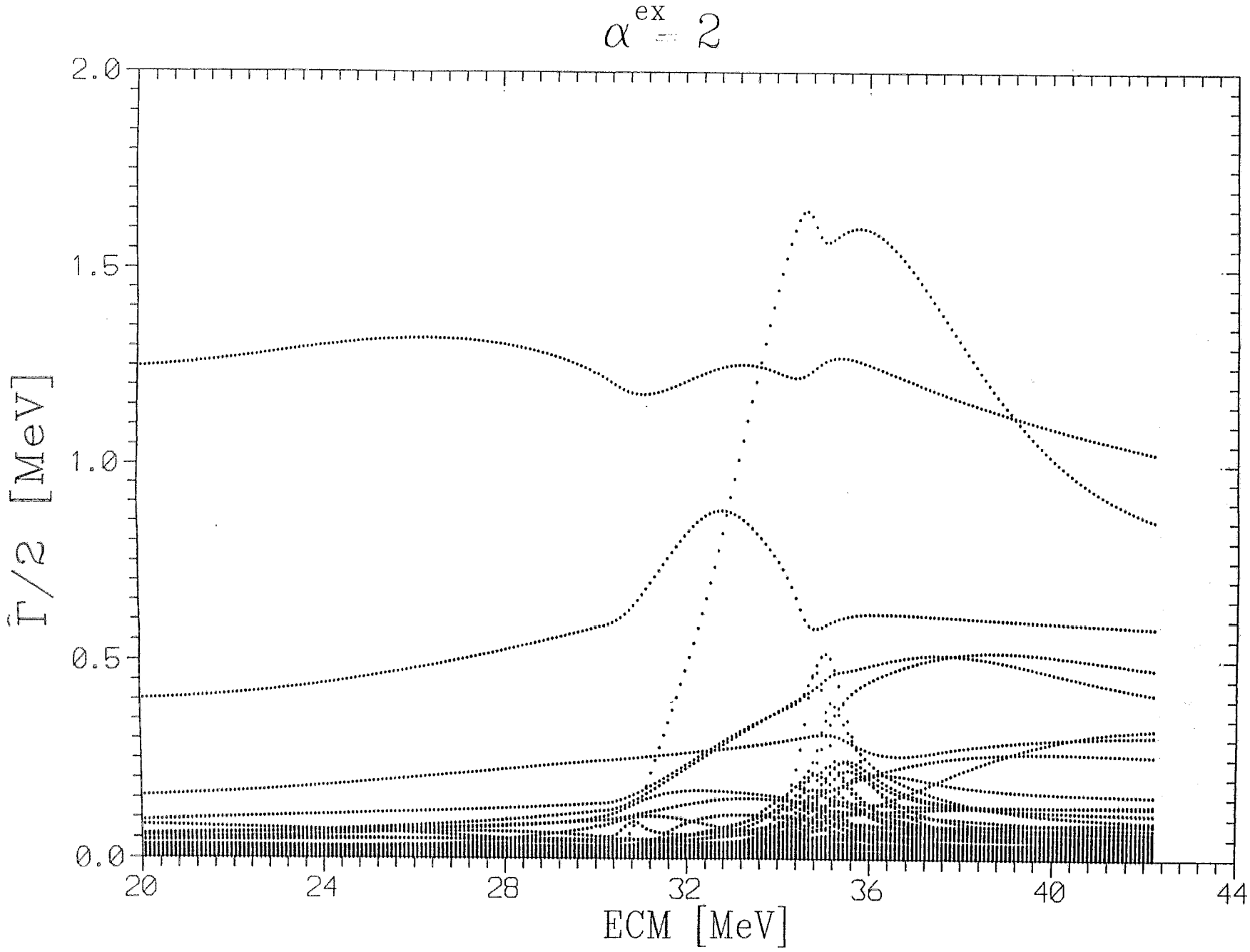
$\alpha^{ex} = 2$
2.0
1.5
1.0
0.5
0.0
Γ/2 [MeV]
20
24
28
32
36
40
44
ECM [MeV]

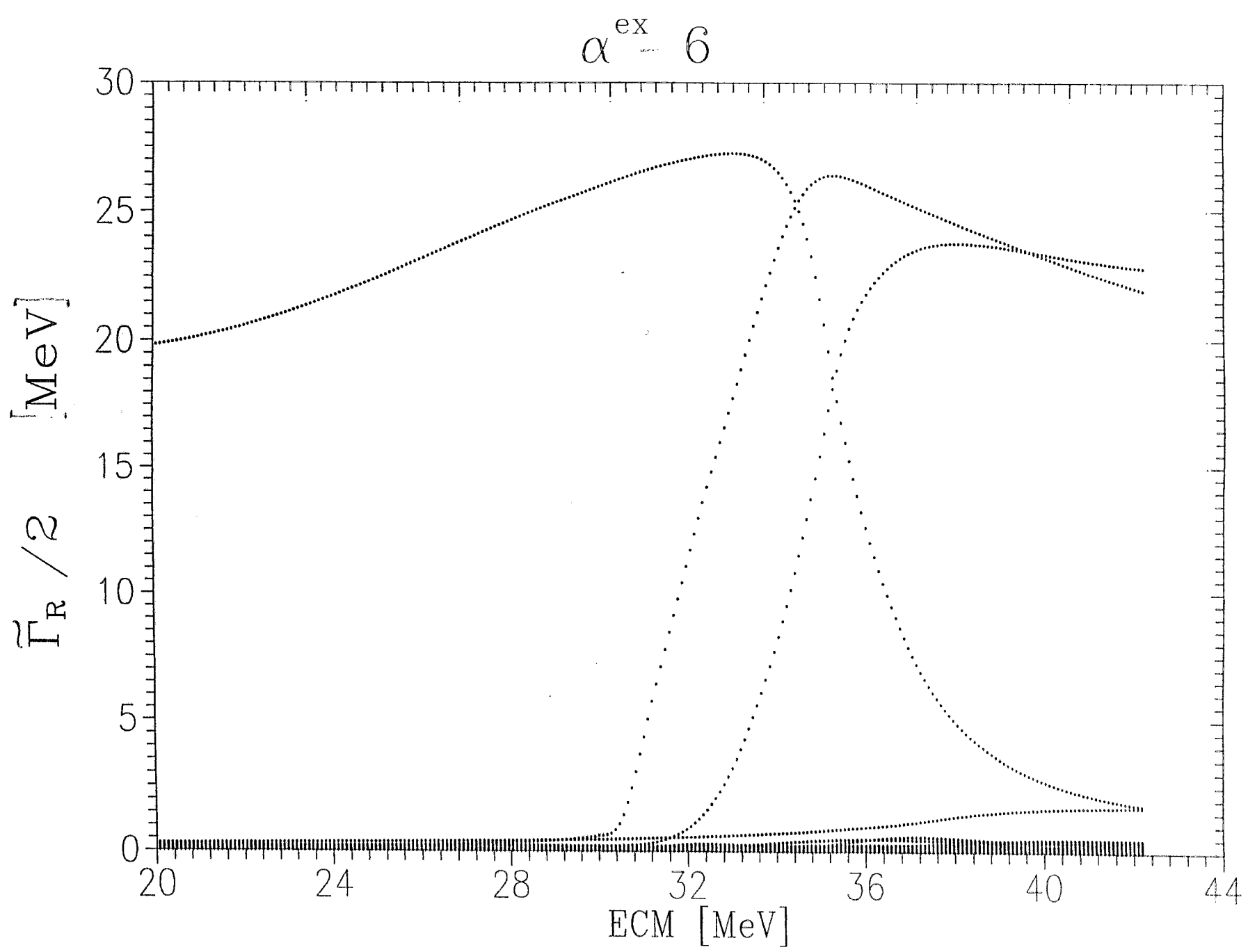
α^{ex} = 6
30
25
20
15
10
5
0
Γ_R /2 [MeV]
20
24
28
32
36
40
44
ECM [MeV]

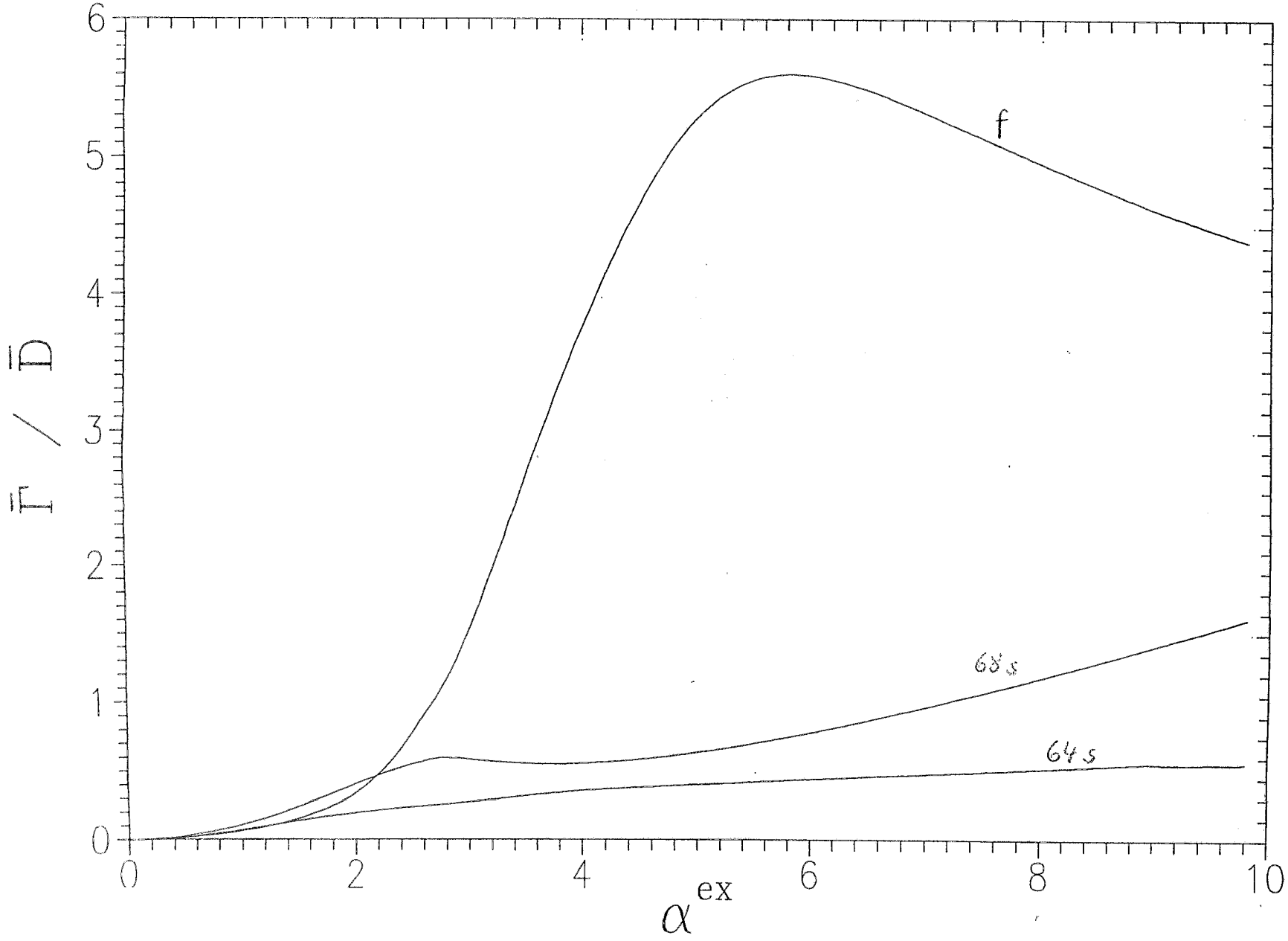
6
5
4
3
2
1
0
0
2
4
6
8
10
f
$6\delta_s$
64_s
$\bar{F} / \bar{D}$
α^{ex}

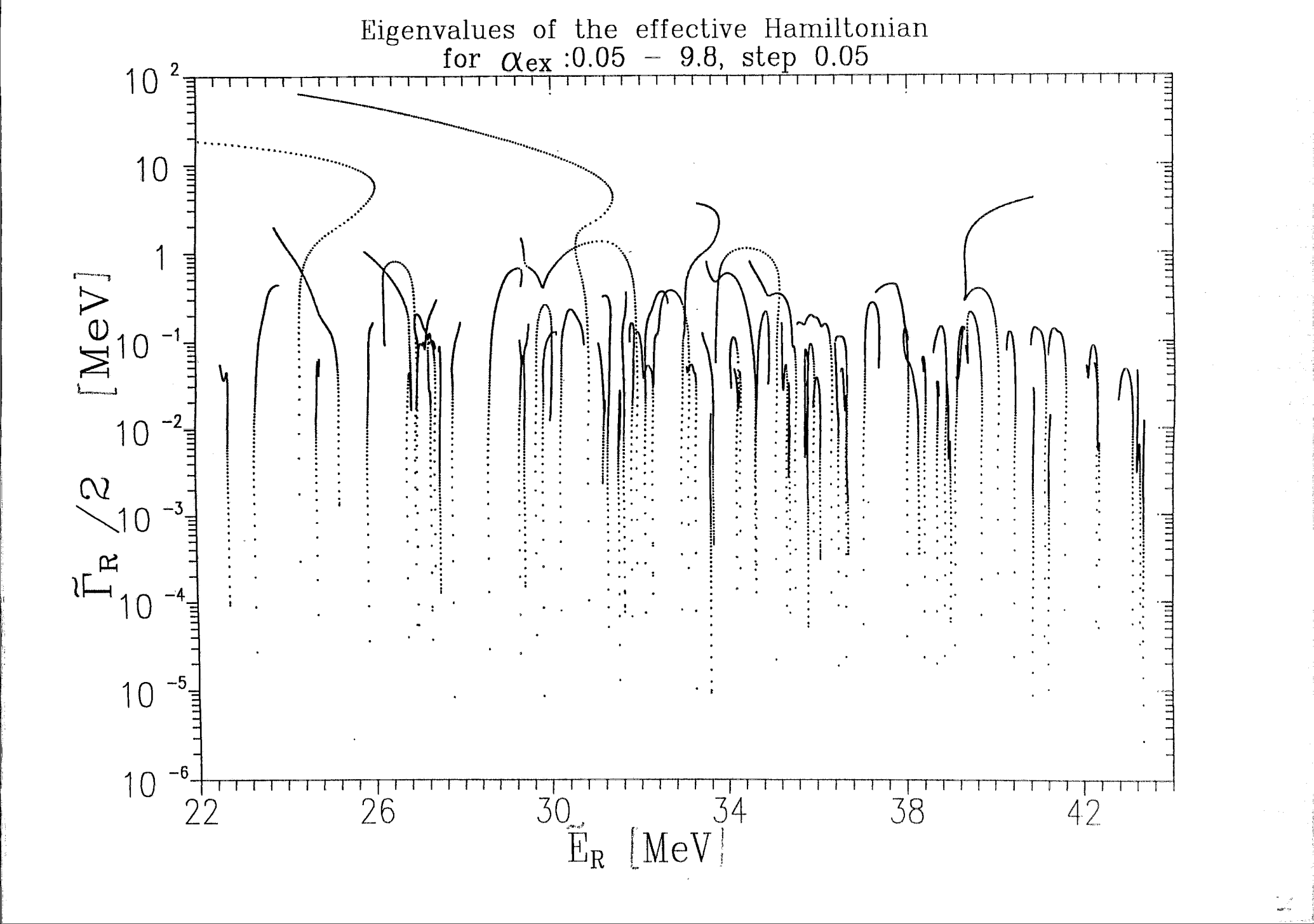
Eigenvalues of the effective Hamiltonian
for α_{ex} :0.05 – 9.8, step 0.05
10^{2}
10
1
10^{-1}
10^{-2}
10^{-3}
10^{-4}
10^{-5}
10^{-6}
$\tilde{\Gamma}_R/2$ [MeV]
22
26
30
34
38
42
$\tilde{E}_R$ [MeV]

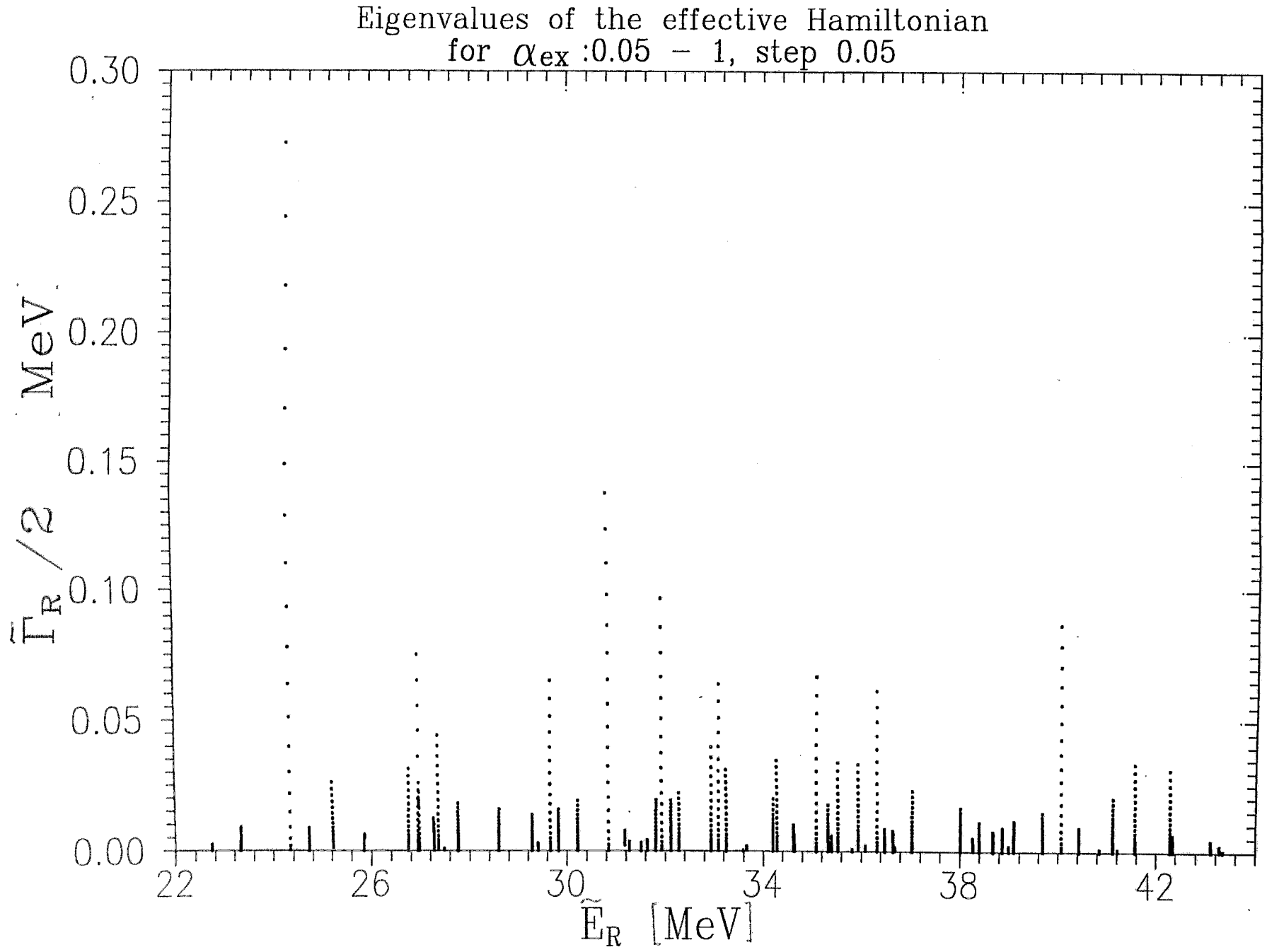
Eigenvalues of the effective Hamiltonian
for α_{ex} :0.05 – 1, step 0.05
0.30
0.25
0.20
0.15
0.10
0.05
0.00
$\tilde{\Gamma}_R/2$ MeV
22
26
30
34
38
42
$\tilde{E}_R$ [MeV]

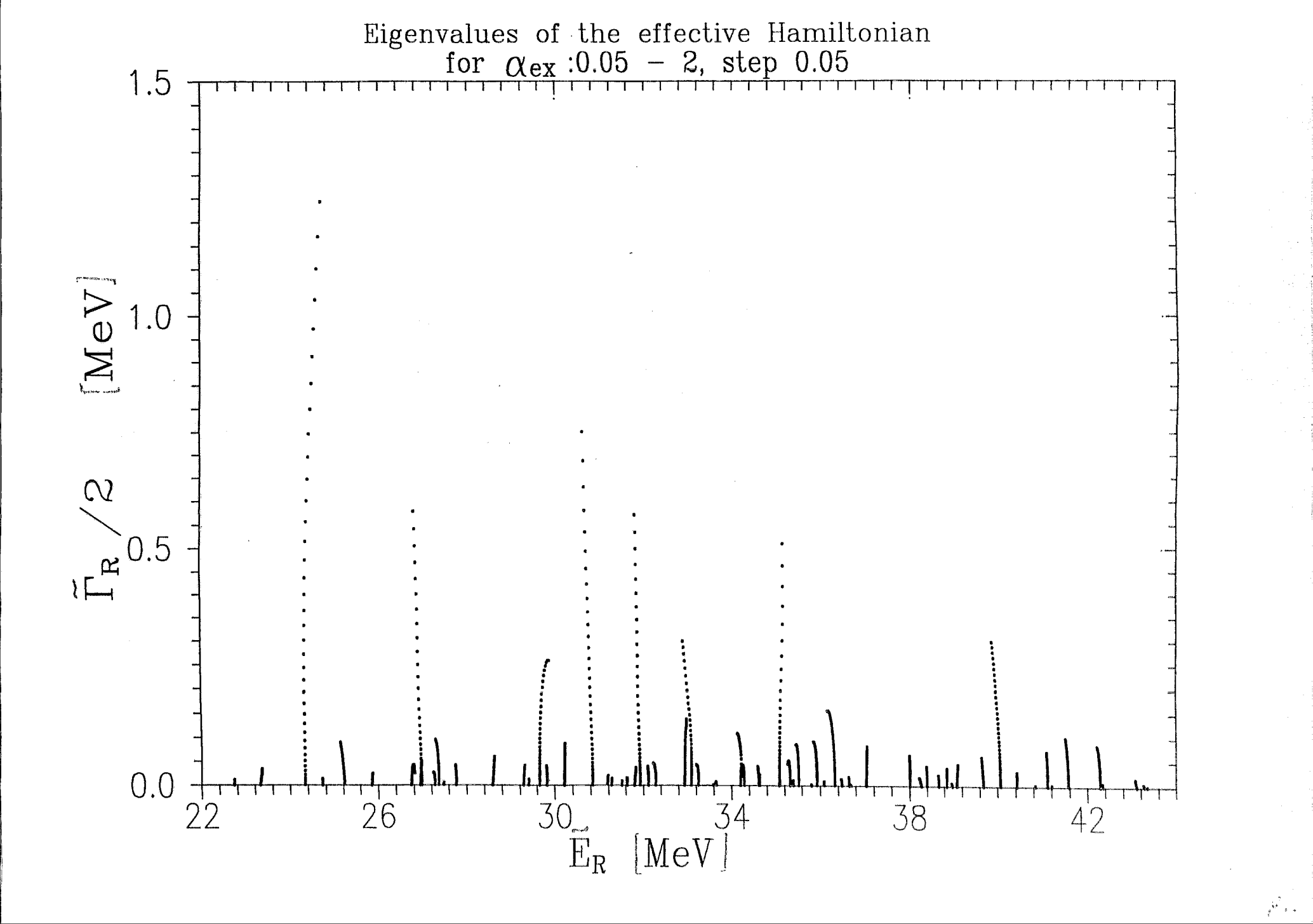
Eigenvalues of the effective Hamiltonian
for α_{ex} :0.05 – 2, step 0.05
1.5
1.0
0.5
0.0
$\tilde{\Gamma}_R/2$ [MeV]
22
26
30
34
38
42
$\tilde{E}_R$ [MeV]

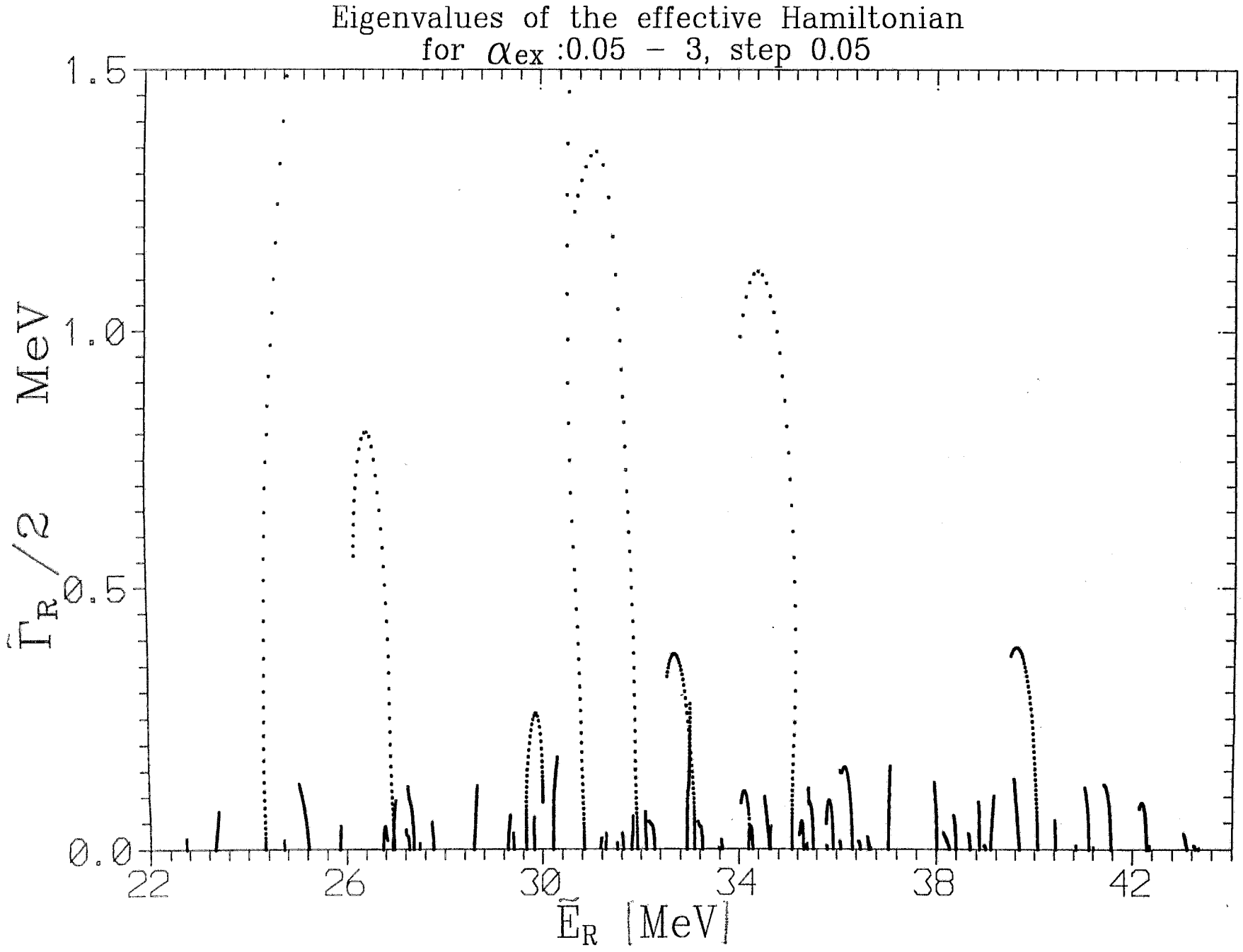
Eigenvalues of the effective Hamiltonian
for α_{ex} :0.05 – 3, step 0.05
1.5
1.0
0.5
0.0
$\tilde{\Gamma}_R/2$ MeV
22
26
30
34
38
42
$\tilde{E}_R$ [MeV]

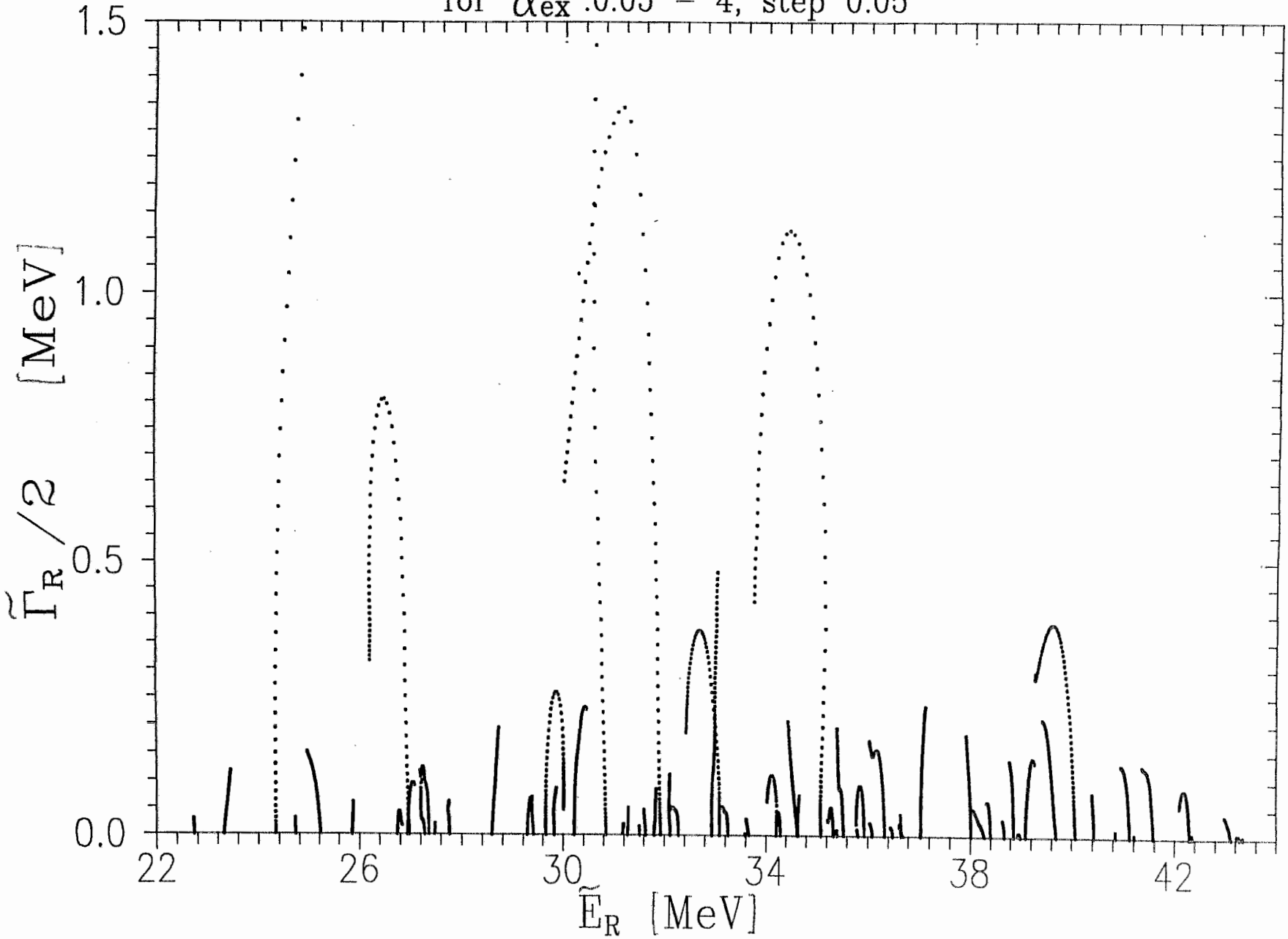
Eigenvalues of the effective Hamiltonian
for α_{ex} :0.05 – 4, step 0.05
1.5
1.0
0.5
0.0
$\tilde{\Gamma}_R/2$ [MeV]
22
26
30
34
38
42
$\tilde{E}_R$ [MeV]

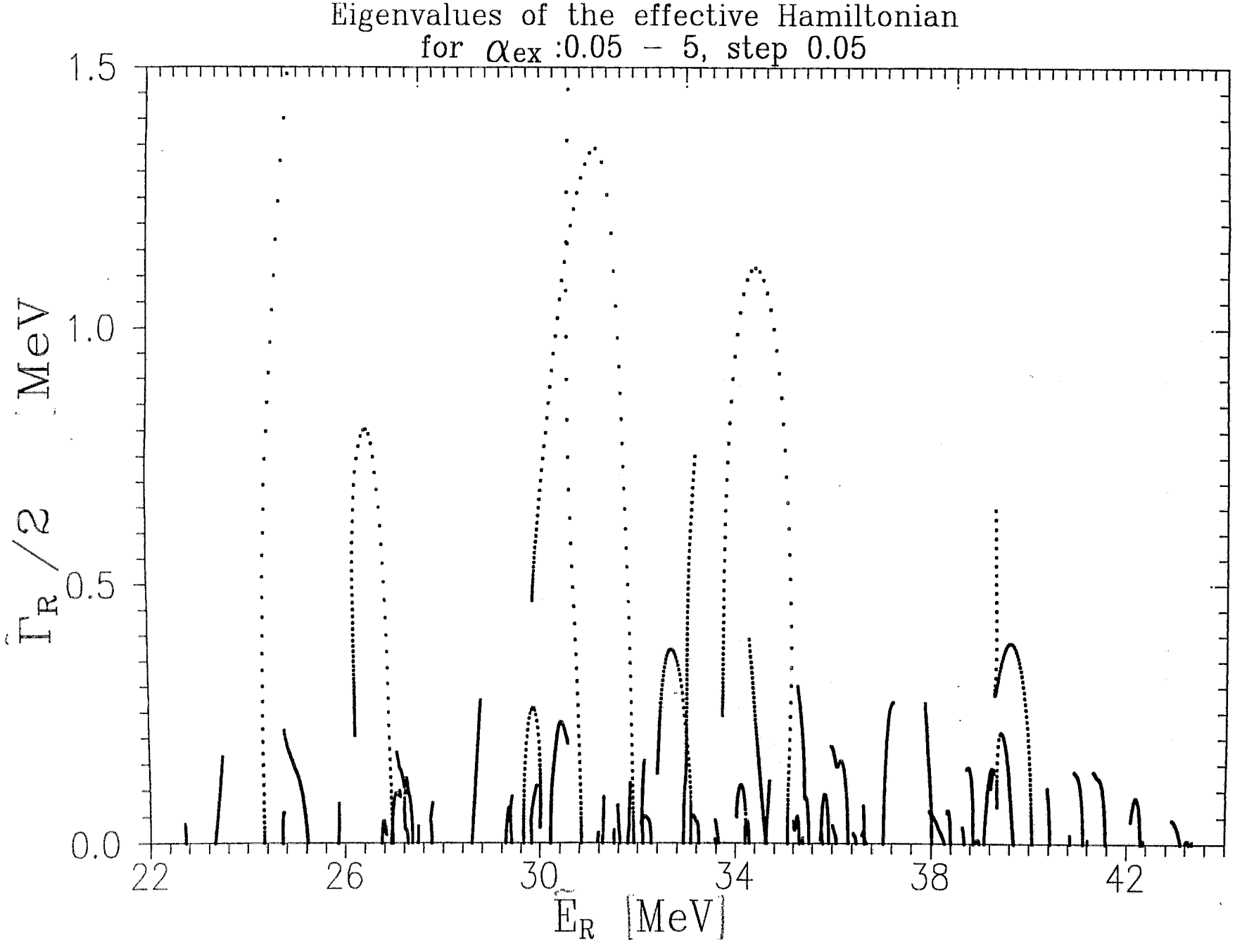
Eigenvalues of the effective Hamiltonian
for α_{ex} :0.05 – 5, step 0.05
1.5
1.0
0.5
0.0
$\tilde{\Gamma}_R/2$ MeV
22
26
30
34
38
42
$\tilde{E}_R$ [MeV]

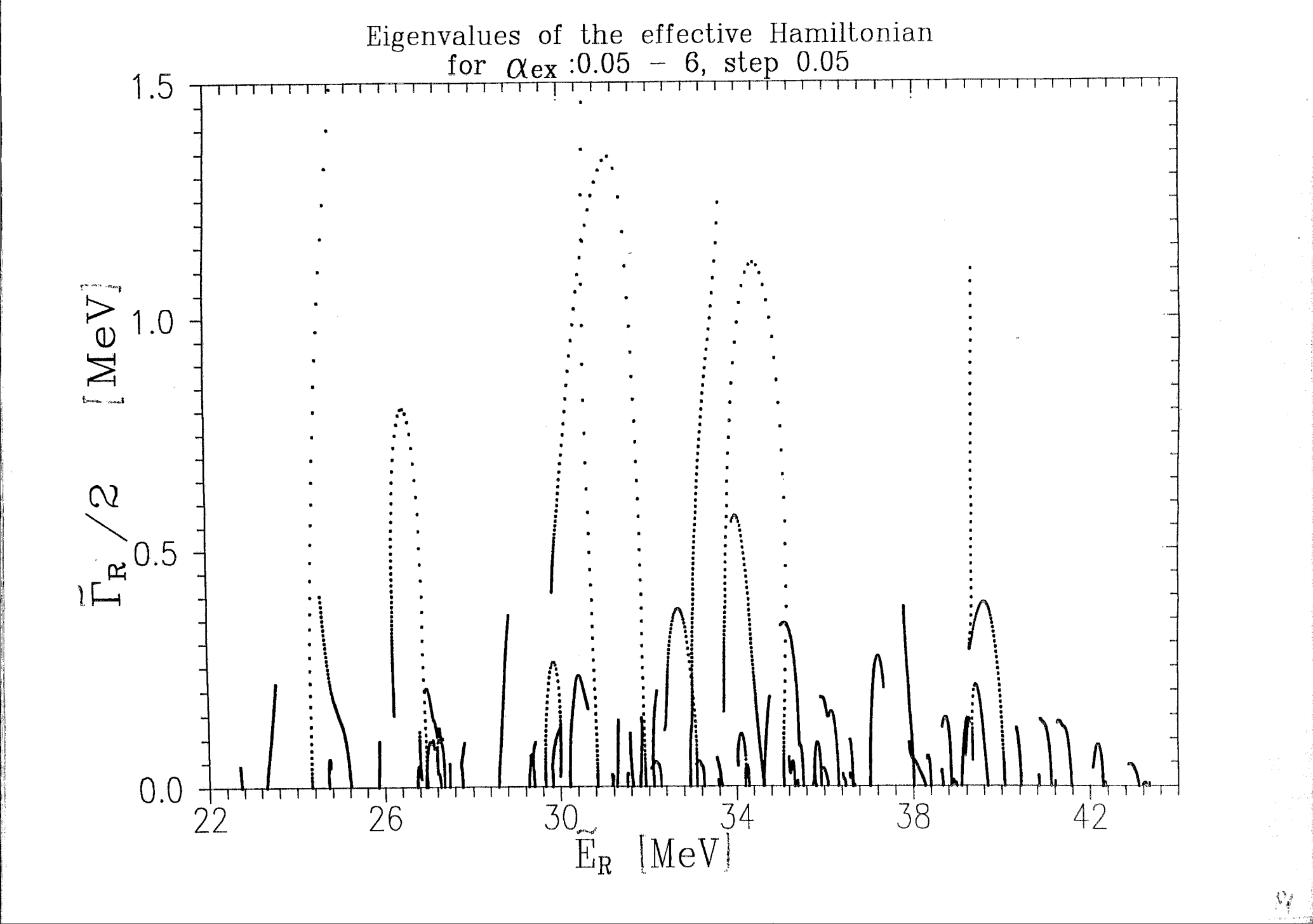
Eigenvalues of the effective Hamiltonian
for α_{ex} :0.05 – 6, step 0.05
1.5
1.0
0.5
0.0
$\tilde{\Gamma}_R/2$ [MeV]
22
26
30
34
38
42
$\tilde{E}_R$ [MeV]

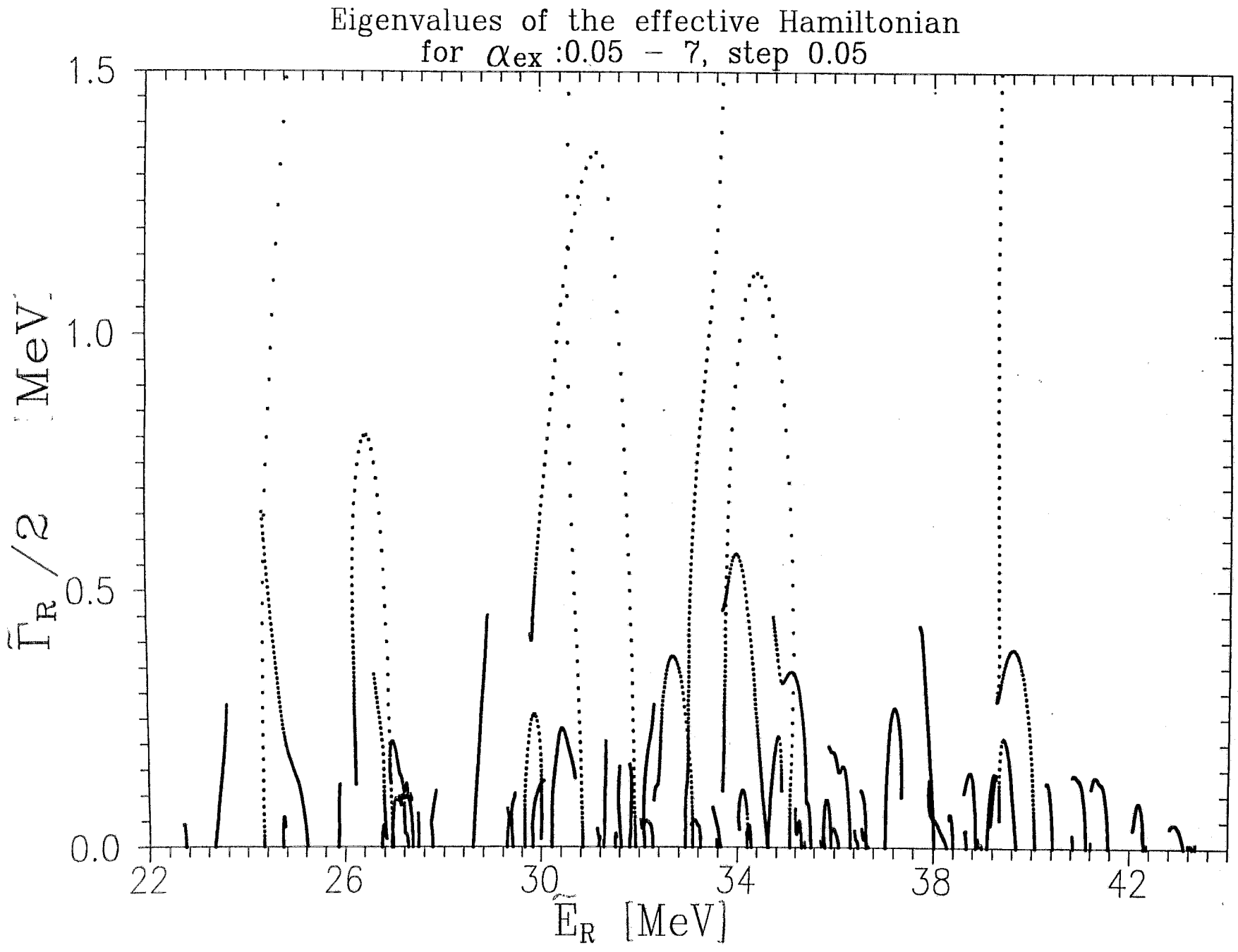
Eigenvalues of the effective Hamiltonian
for α_{ex} :0.05 – 7, step 0.05
1.5
1.0
0.5
0.0
$\tilde{\Gamma}_R/2$ MeV
22
26
30
34
38
42
$\tilde{E}_R$ [MeV]

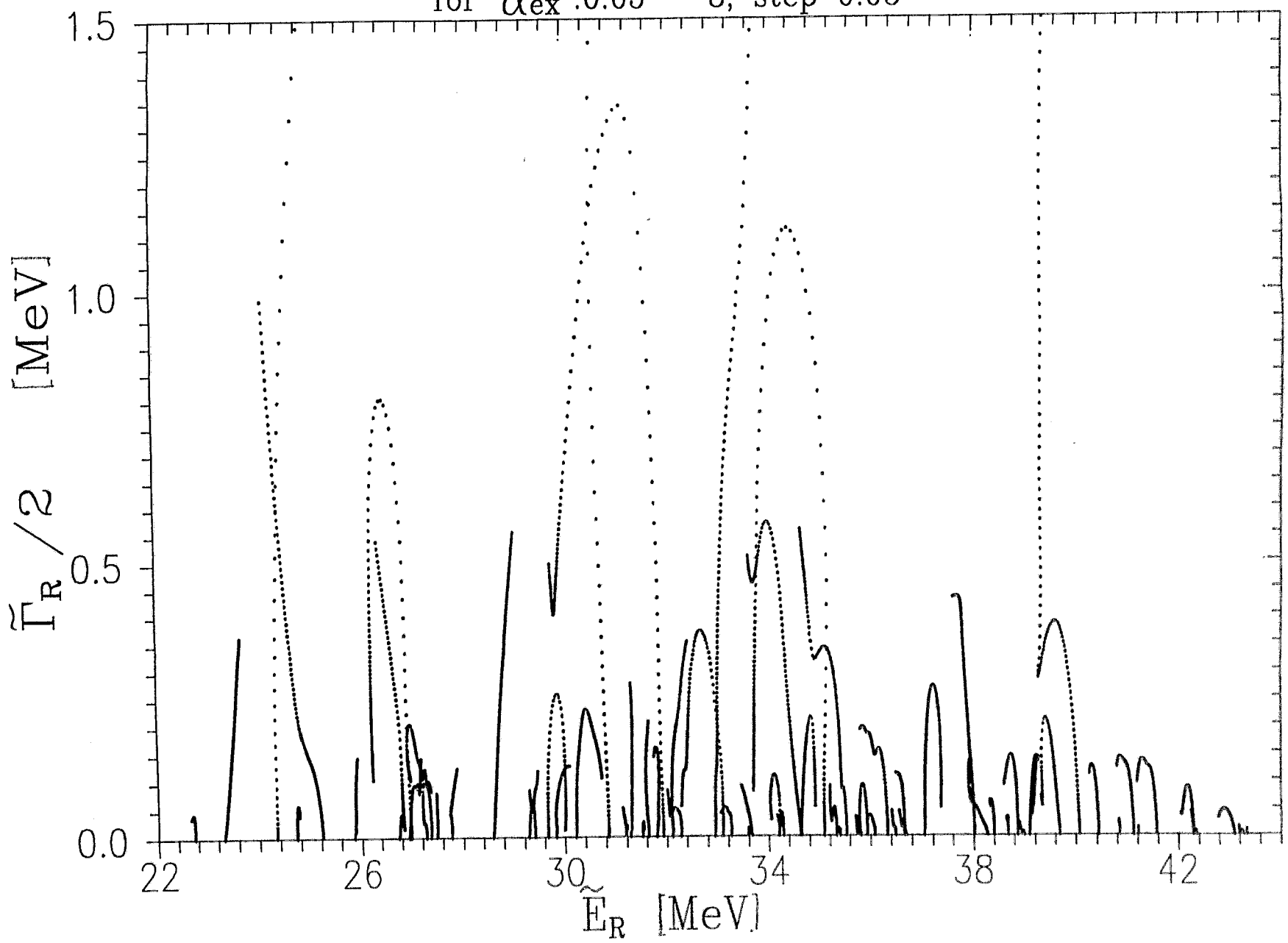
Eigenvalues of the effective Hamiltonian
for α_{ex} :0.05 – 8, step 0.05
1.5
1.0
0.5
0.0
$\tilde{\Gamma}_R/2$ [MeV]
22
26
30
34
38
42
$\tilde{E}_R$ [MeV]